Electroweak single pion production

RGJ, UCM

Neutrini and nuclei, challenges and opportunities for nuclear theory, ECT*, Trento, Italy, 27-31 May, 2019

Electroweak single pion production

Raúl González Jiménez

**Nuclear Physics Group,
Complutense University of Madrid, Spain**

*Neutrini and nuclei, challenges and opportunities for nuclear theory,
ECT*, Trento, Italy, 27-31 May, 2019*

Collaborators

Ghent University

Natalie Jachowicz

Kajetan Niewczas

Alexis Nikolakopoulos

Jannes Nys

Vishvas Pandey

Tom Van Cuyck

Nils Van Dessel

Complutense University

Jose Manuel Udías

Wroclaw University

Kajetan Niewczas

Jan Sobczyk

Outline

I Introduction

II Interaction model: From low to high

III Nuclear effects (RMF model)

IV Conclusions

What we know from (e,e')

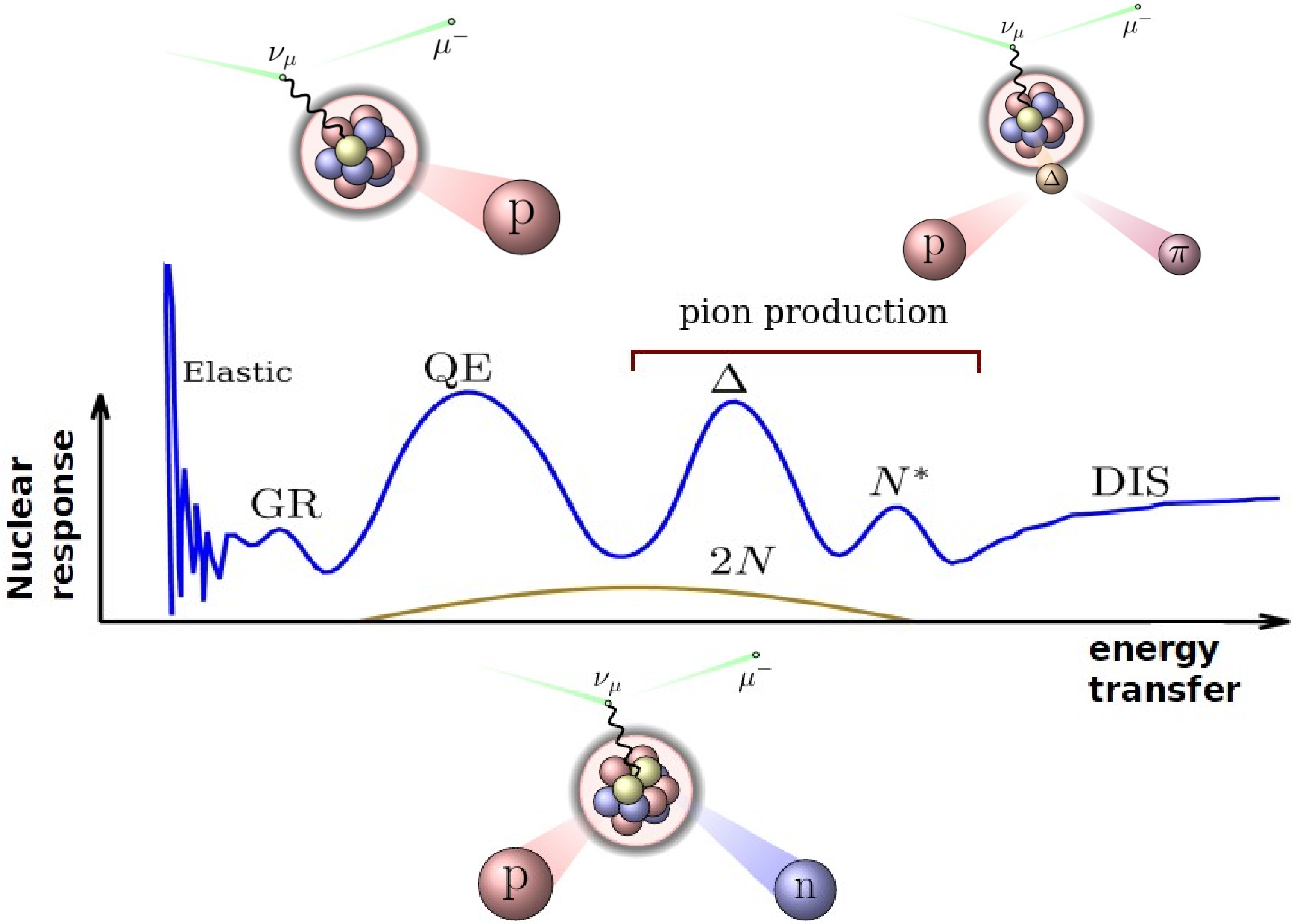

Figures by T. Van Cuyck

Why pion production?

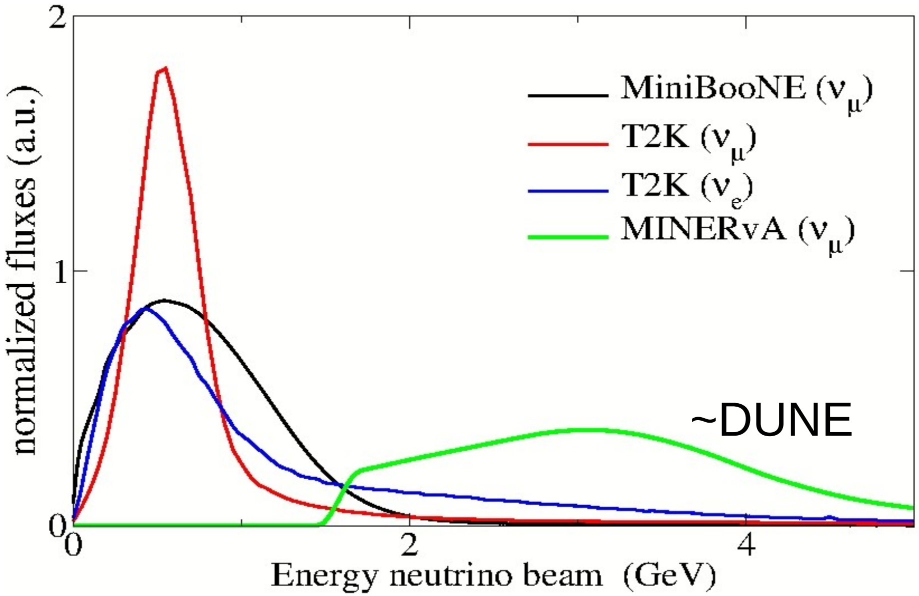

Pion production will be one of the main contributions in DUNE

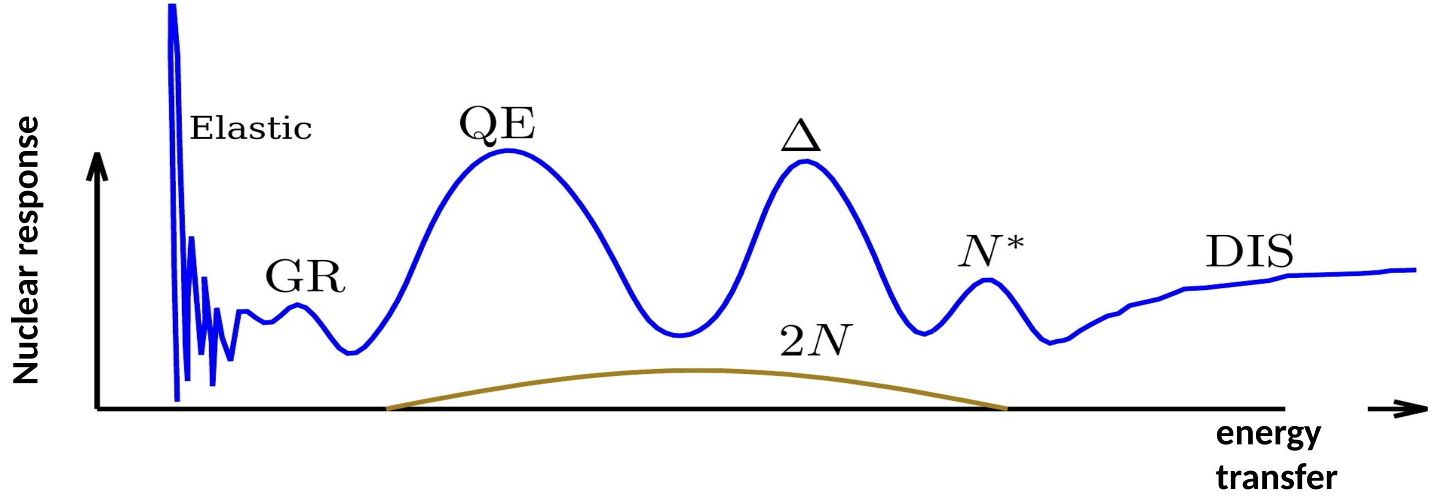

II Interaction model

Single-Pion Production off the nucleon

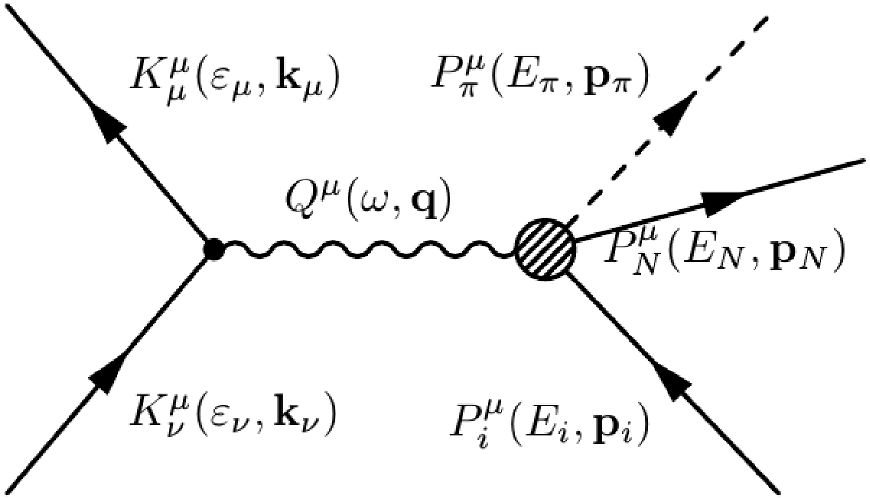

RGJ et al., PRD 95, 113007 (2017)

Low-energy model

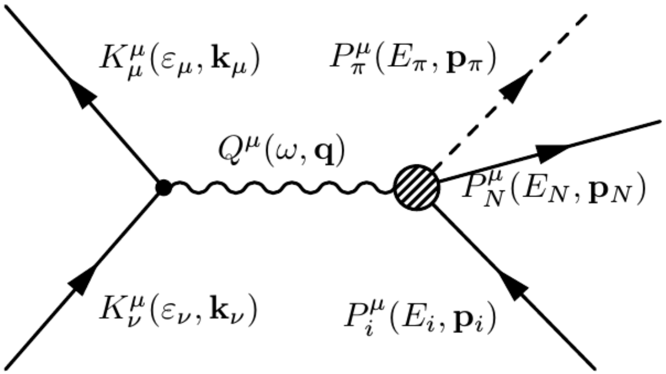

Low-energy model for pion-production on the nucleon:

ChPT background + resonances

Valencia model

(PRD 76 (2007) 033005; PRD 87 (2013) 113009)

Resonances:

P33(1232), D13(1520),
S11(1535), P11(1440)

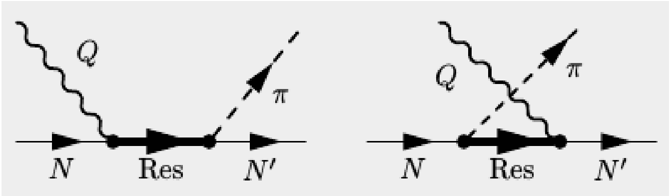

ChPT background:

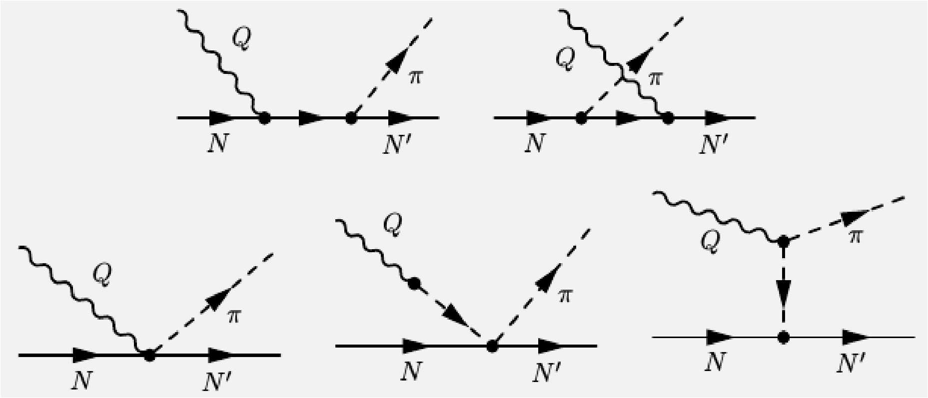

Low-energy model

PHYSICAL REVIEW D **98,** 073001 (2018)

Angular distributions in electroweak pion production off nucleons: Odd parity hadron terms, strong relative phases, and model dependence

J. E. Sobczyk,[1] E. Hernández,[2] S. X. Nakamura,[3] J. Nieves,[1] and T. Sato[4]

[1]*Instituto de Física Corpuscular (IFIC), Centro Mixto CSIC-Universidad de Valencia, Institutos de Investigación de Paterna, Apartado 22085, E-46071 Valencia, Spain*

[2]*Departamento de Física Fundamental e IUFFyM, Universidad de Salamanca, E-37008 Salamanca, Spain*

[3]*Laboratório de Física Teórica e Computacional-LFTC, Universidade Cruzeiro do Sul, São Paulo, SP, 01506-000, Brazil*

[4]*RCNP, Osaka University, Ibaraki, Osaka 567-0047, Japan*

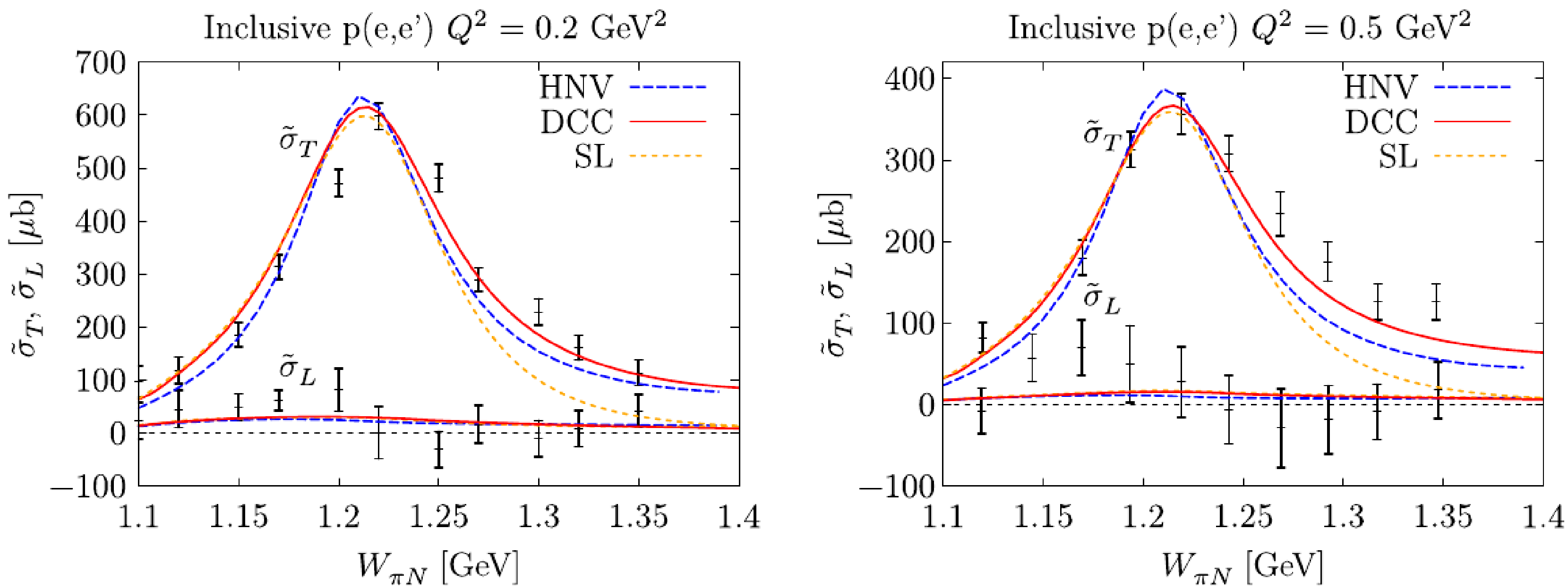

PRD98, 073001 (2018)

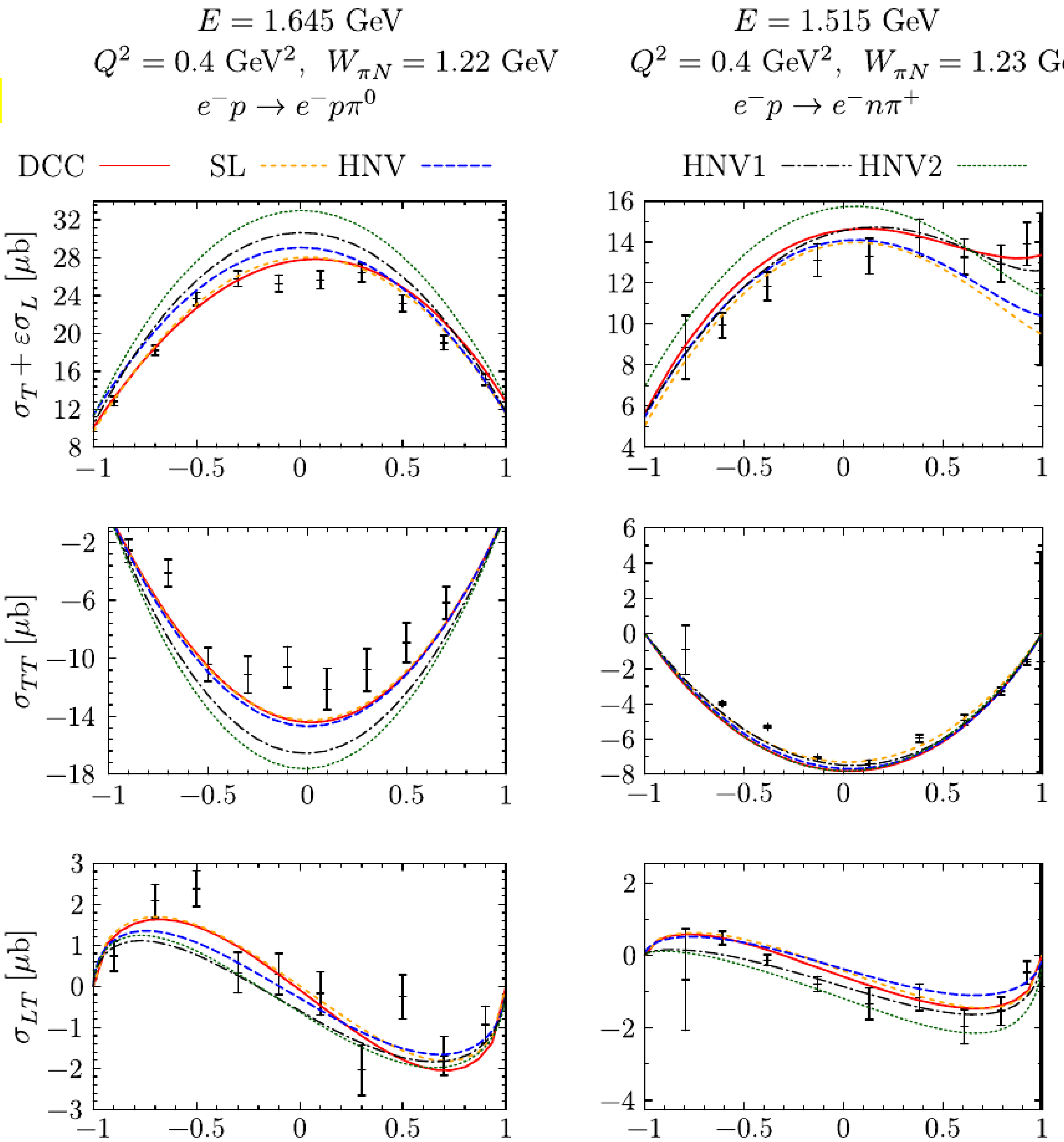

A problem

Unphysical predictions at large invariant masses.

p(e,e')X

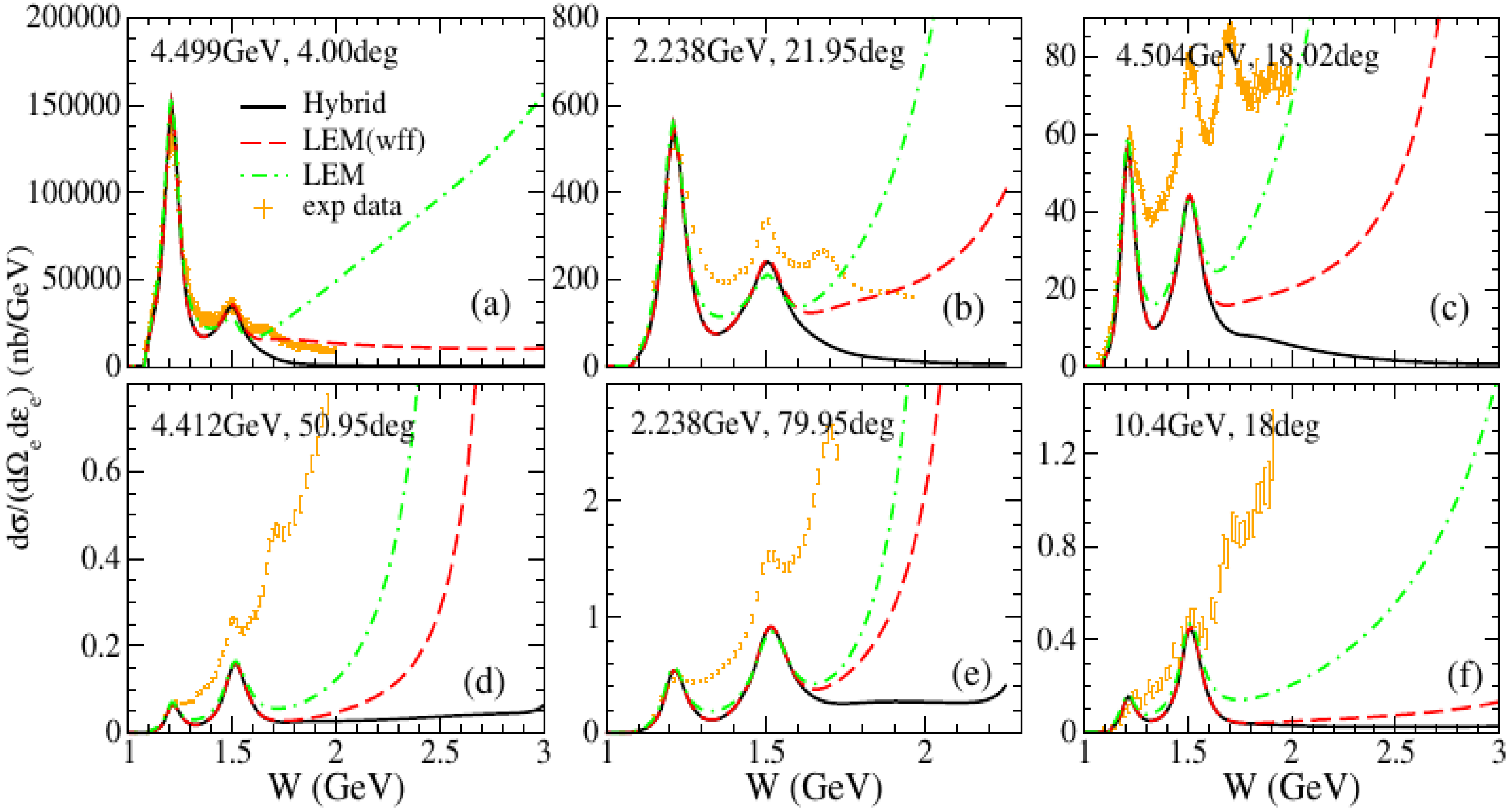

Figure: The model overshoots **inclusive electron-proton** scattering data.

Does it matter for neutrinos?

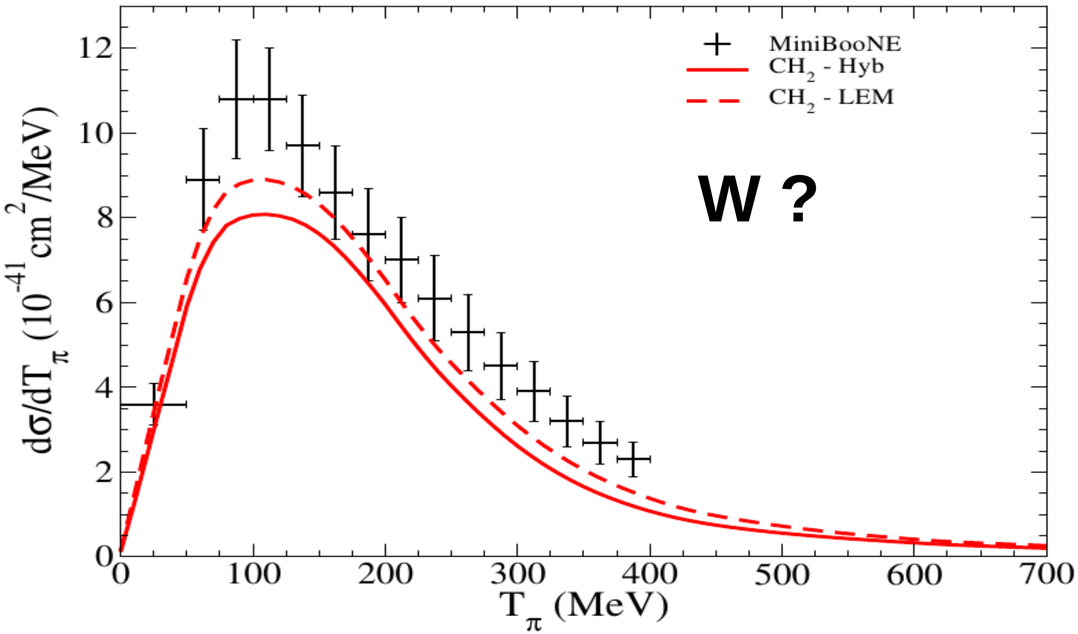

Invariant mass (W) values?

- **+** Fermi motion
- **+** Flux-folding

Therefore, one needs reliable predictions in:

- **+** the **resonance region** W < 2 GeV,
- **+** the **high-energy** energy region W > 2 GeV

The Problem

The pathologies come from the

resonances and **background terms**

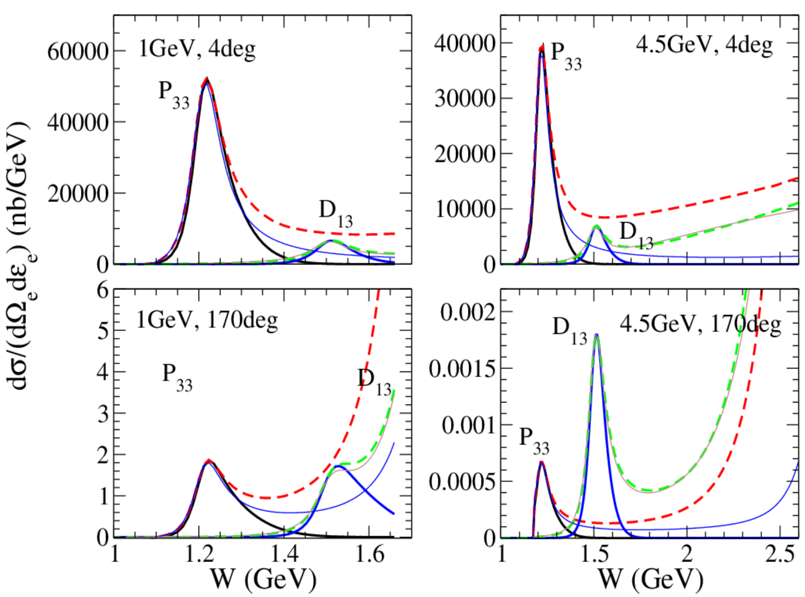

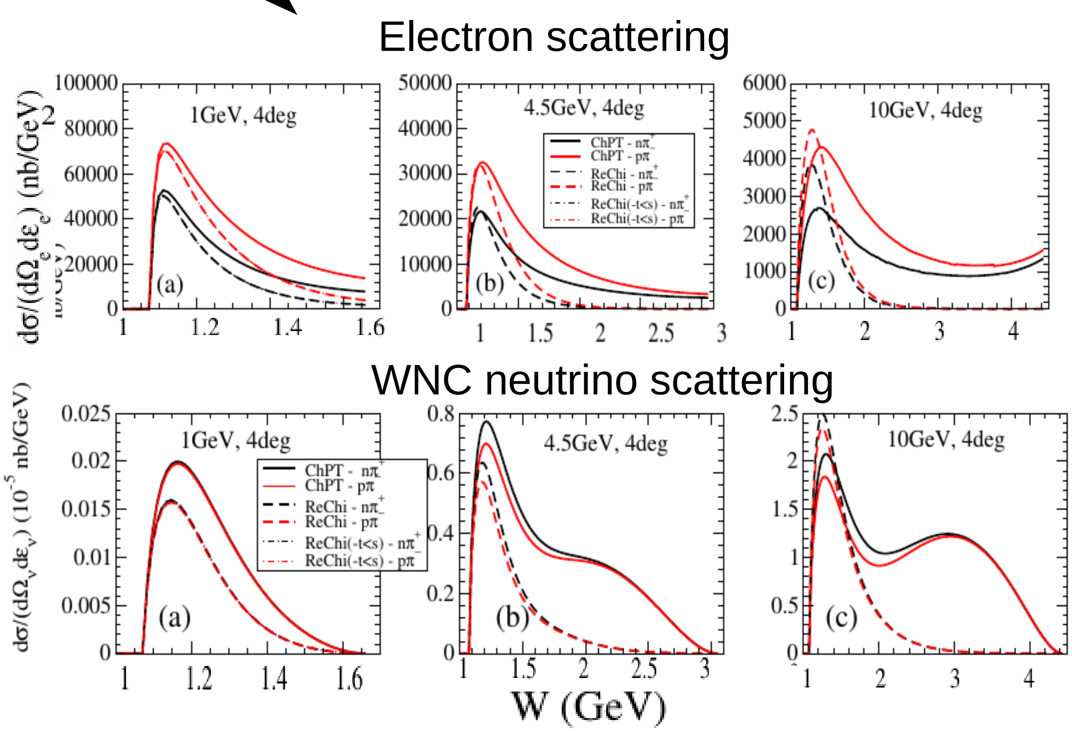

Why does this happen?

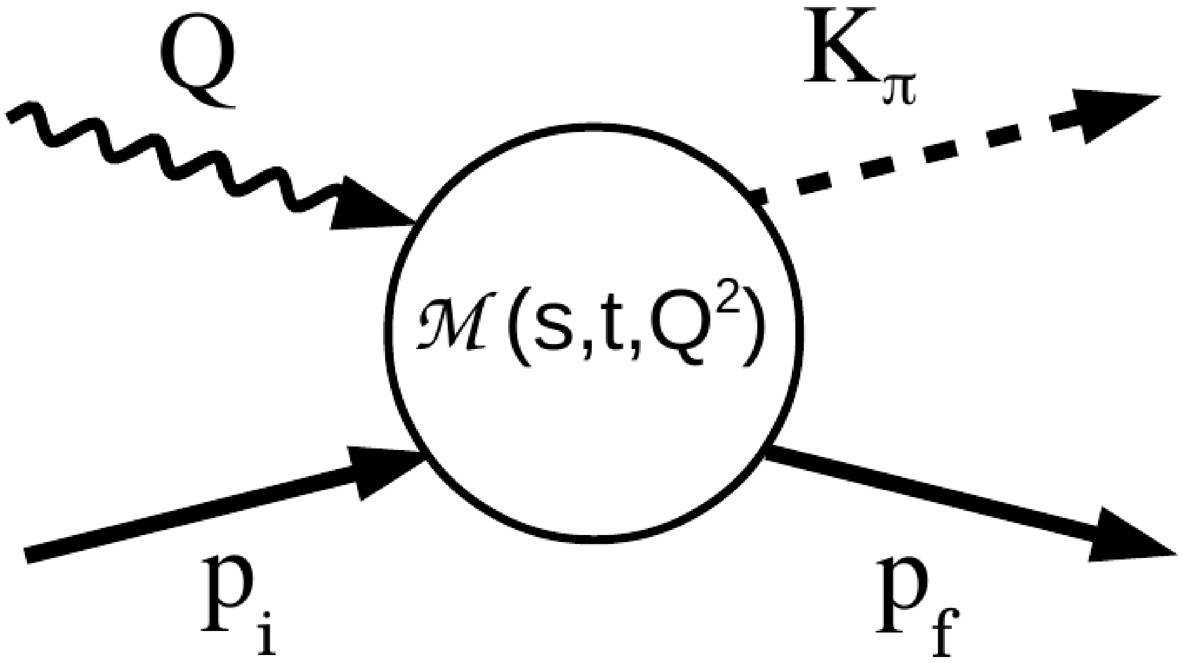

Direct channels

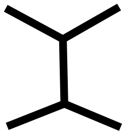

Cross channels

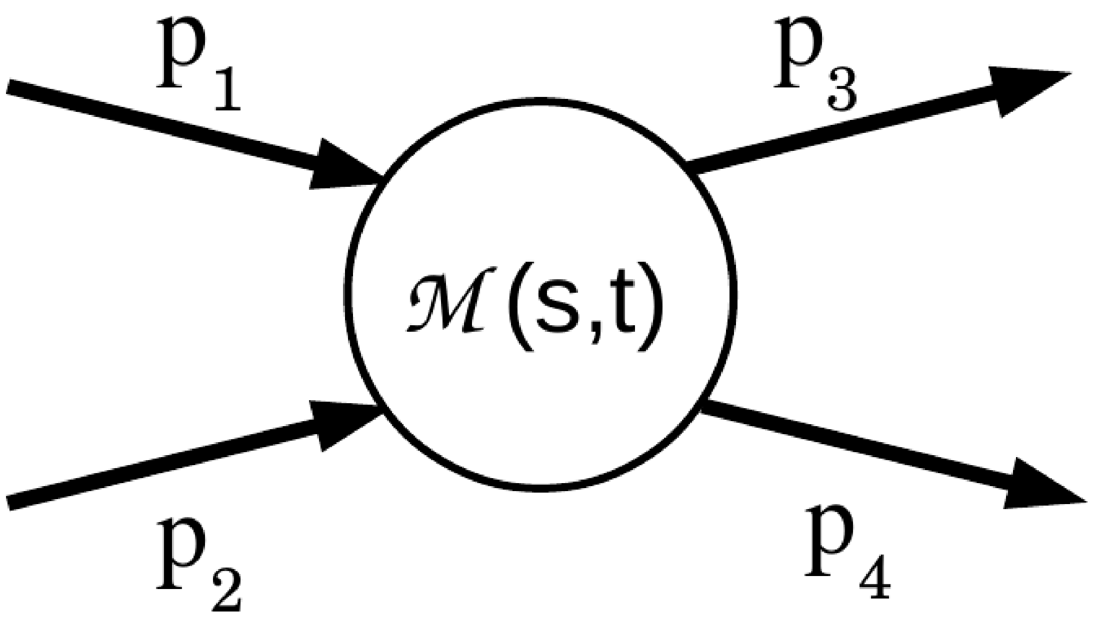

$s = (p_1+p_2)^2$ $t = (p_1-p_3)^2$ $u = (p_1-p_4)^2$

$$s + t + u = 4m^2$$

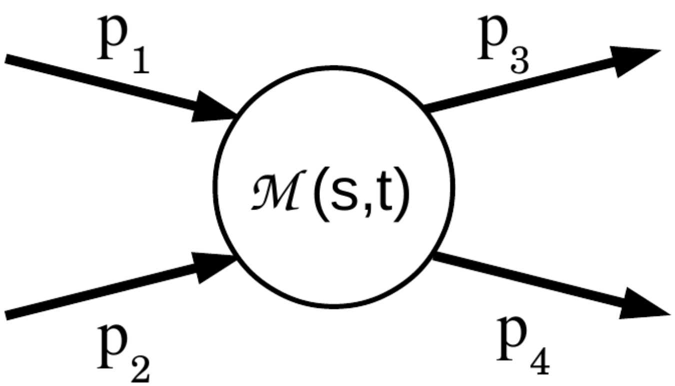

$$s + t + u = 4m^2$$

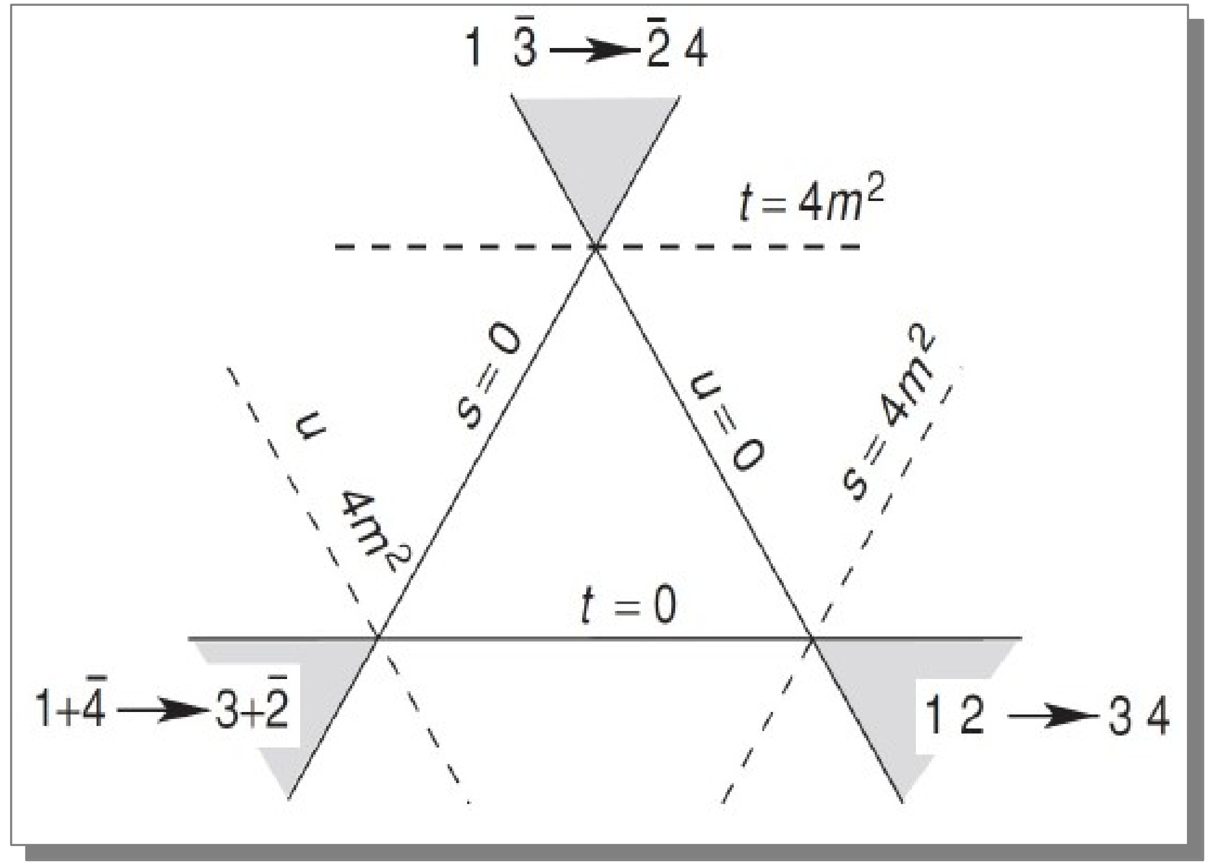

$$p_1+p_2 \rightarrow p_3+p_4 \qquad \textbf{Crossing Symmetry} \qquad p_1+\overline{p}_3 \rightarrow \overline{p}_2+p_4$$

$$M_s(s,t) = M_t(t,s)$$

Why does this happen?

Cross channels: 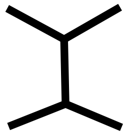

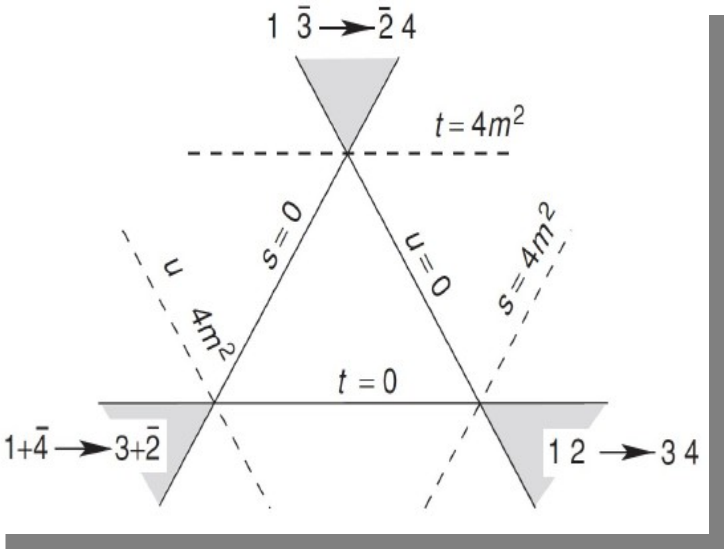

$$\mathcal{A}(t,s) = \sum_\ell (2\ell+1)\, A_\ell(t)\, P_\ell(z_t)$$

$$z_t \equiv 1 + \frac{2s}{t-4m^2}$$

$$P_\ell(z_t) \xrightarrow{s\to\infty} (2s)^\ell$$

Infinite for s → ∞ !!

Why does this happen?

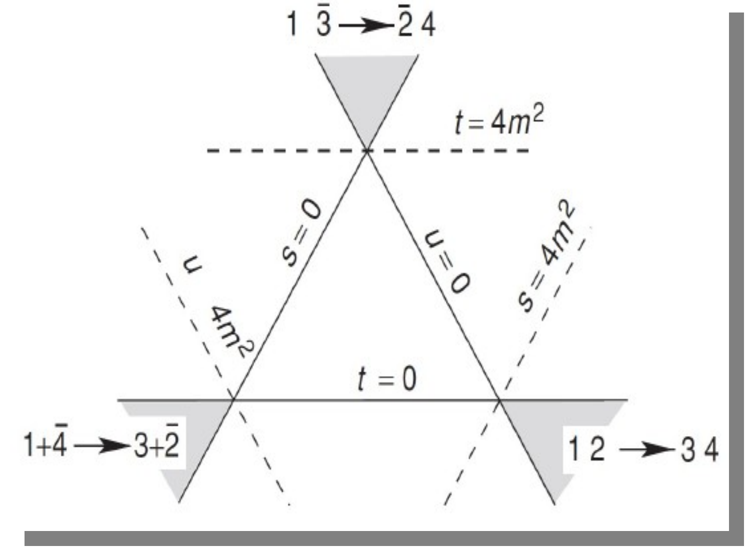

Direct channels: 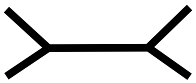

$$\mathcal{A}(s,t) = \sum_{\ell} (2\ell + 1)\, A_\ell(s)\, P_\ell(z_s)$$

$$z_s \equiv \cos\theta_s = 1 + \frac{2t}{s - 4m^2}$$

$$A_\ell(s) \sim \left(\frac{s - 4m^2}{2}\right)^{\ell}$$

Behavior at threshold (barrier factor).
Feynman diagrams provide the right behavior at threshold but not at high s

Infinite for s $\to \infty$!!

Regge Theory

$$\mathcal{A}(t,s) = \sum_{\ell} (2\ell + 1)\, A_\ell(t)\, P_\ell(z_t)$$

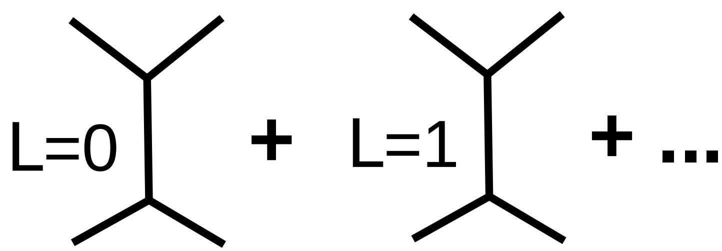

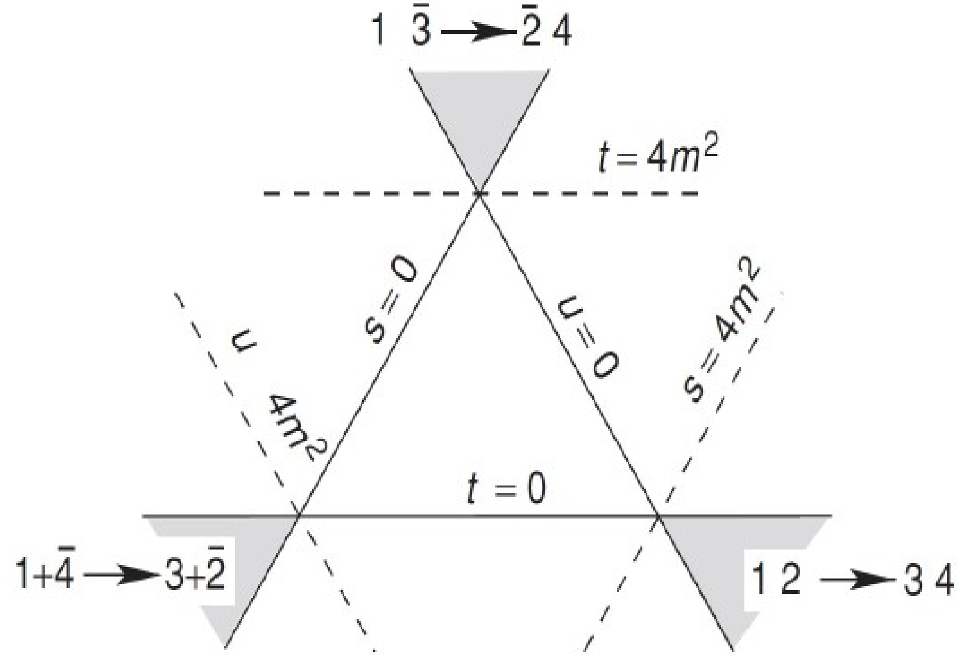

Regge Theory

$$\mathcal{M}(s,t) = -\frac{1}{2i}\oint_{C_1} d\lambda \frac{(2\lambda+1)\,\mathcal{M}_\lambda(t)\,P_\lambda(-\cos\theta_t)}{\sin(\pi\lambda)}$$

Regge limit:
* Large **s**
* Small negative **t**

$$\mathcal{M}^{\zeta}_{\text{Regge}}(s,t) = C\sum_i \left(\frac{s}{s_0}\right)^{\alpha_i^\zeta(t)} \frac{\beta_i^\zeta(t)}{\sin\left(\pi\alpha_i^\zeta(t)\right)} \frac{1+\zeta e^{-i\pi\alpha_i^\zeta(t)}}{2} \frac{1}{\Gamma\left(\alpha_i^\zeta(t)+1\right)} .$$

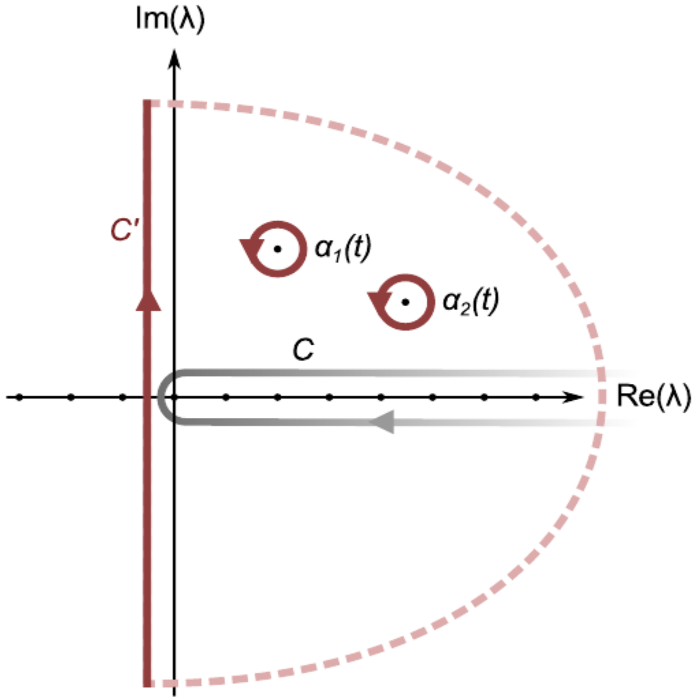

Image from
L. De Cruz, PhD Thesis.
Ghent University

Regge Theory

Based on unitarity, causality and crossing symmetry, Regge Theory provides the **high energy ($s \rightarrow \infty$) behavior** of the amplitude:

$$A(s,t) \sim \beta(t)\, s^{\alpha(t)}$$

Regge theory does not predict the **t-dependence** of the amplitude.

For that, one needs a model.

$\alpha(t)$: Families or Regge trajectories

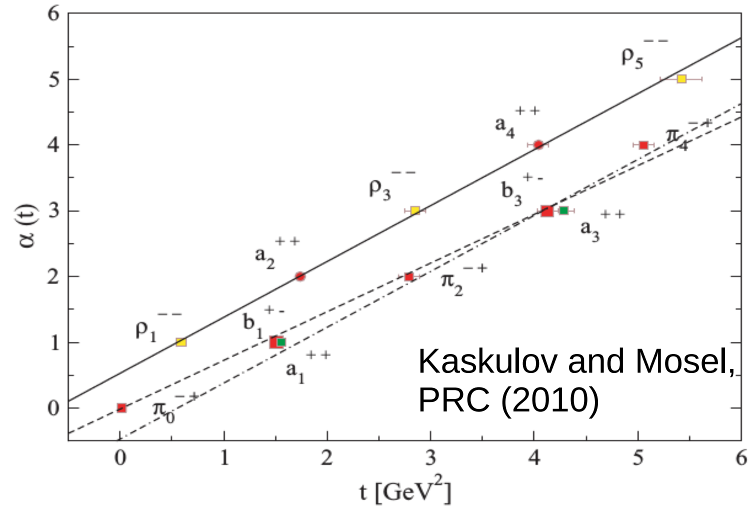

High-energy model

Regge approach for the vector amplitudes.

We use the same approach as **Guidal, Laget, and Vanderhaeghen** [NPA627, 645 (1997)], originally developed for pion photoproduction ($Q^2 = 0$):

1) Feynman **meson-exchange diagrams** are reggeized.

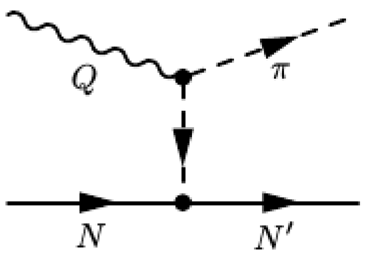

$$\frac{1}{t - m_\pi^2}$$

The pion propagator is replace by the Regge trajectory of the pion family

$$\mathcal{P}_\pi(t,s) = -\alpha'_\pi \varphi_\pi(t)\Gamma[-\alpha_\pi(t)](\alpha'_\pi s)^{\alpha_\pi(t)}$$

High-energy model

Regge approach for the vector amplitudes.

We use the same approach as **Guidal, Laget, and Vanderhaeghen** [NPA627, 645 (1997)], originally developed for pion photoproduction ($Q^2 = 0$):

1) Feynman **meson-exchange diagrams** are reggeized.

2) s-channel and u-channel diagrams are included to keep **Conservation of Vector Current**.

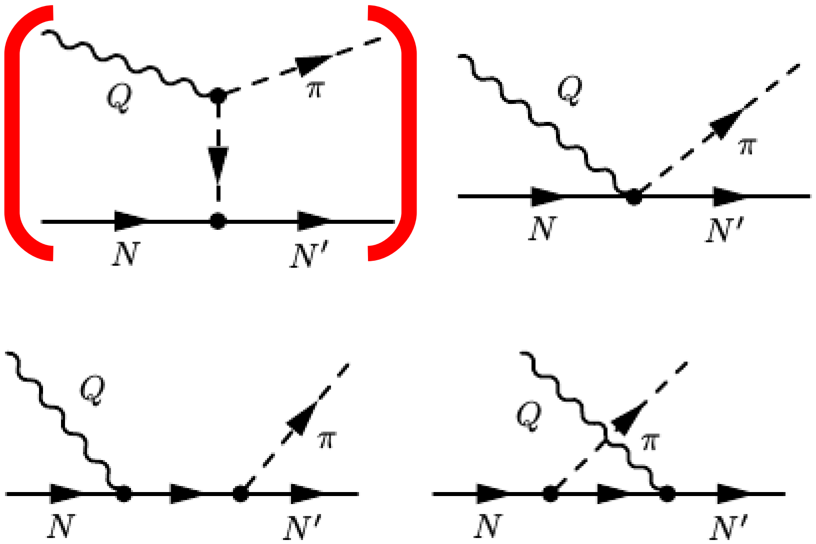

$$\frac{1}{t - m_\pi^2}$$

The pion propagator is replace by the Regge trajectory of the pion family

$$\mathcal{P}_\pi(t,s) = -\alpha'_\pi \varphi_\pi(t) \Gamma[-\alpha_\pi(t)] (\alpha'_\pi s)^{\alpha_\pi(t)}$$

High-energy model

Regge approach for the vector amplitudes.

We use the same approach as **Kaskulov and Mosel** [PRC81, 045202 (2010)], that allows one to extends GLV to the case of pion electroproduction ($Q^2 \neq 0$).

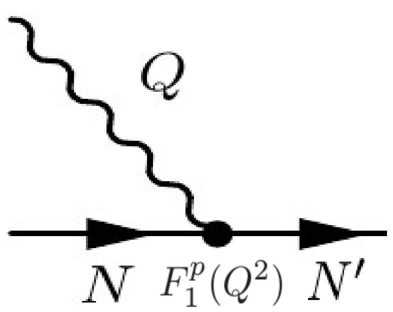

The nucleon N' may be highly off its mass shell.
Therefore, instead of using the on shell form factor $F_1^p(Q^2)$.
We use a form factor that accounts for the off shell character of the nucleon [**Vrancx and Ryckebusch**, PRC89, 025203 (2014)]:

$$F_1^p(Q^2, s) = \left(1 + \frac{Q^2}{\Lambda_{\gamma pp^*}(s)^2}\right)^{-2}$$

$$\Lambda_{\gamma pp^*}(s) = \Lambda_{\gamma pp} + (\Lambda_\infty - \Lambda_{\gamma pp})\left(1 - \frac{M^2}{s}\right)$$

$$\Lambda_\infty = 2.194 \text{ GeV}$$

In the (on shell) limit the Dirac form factor is recovered.

High-energy model: N(e, e'π)N' results

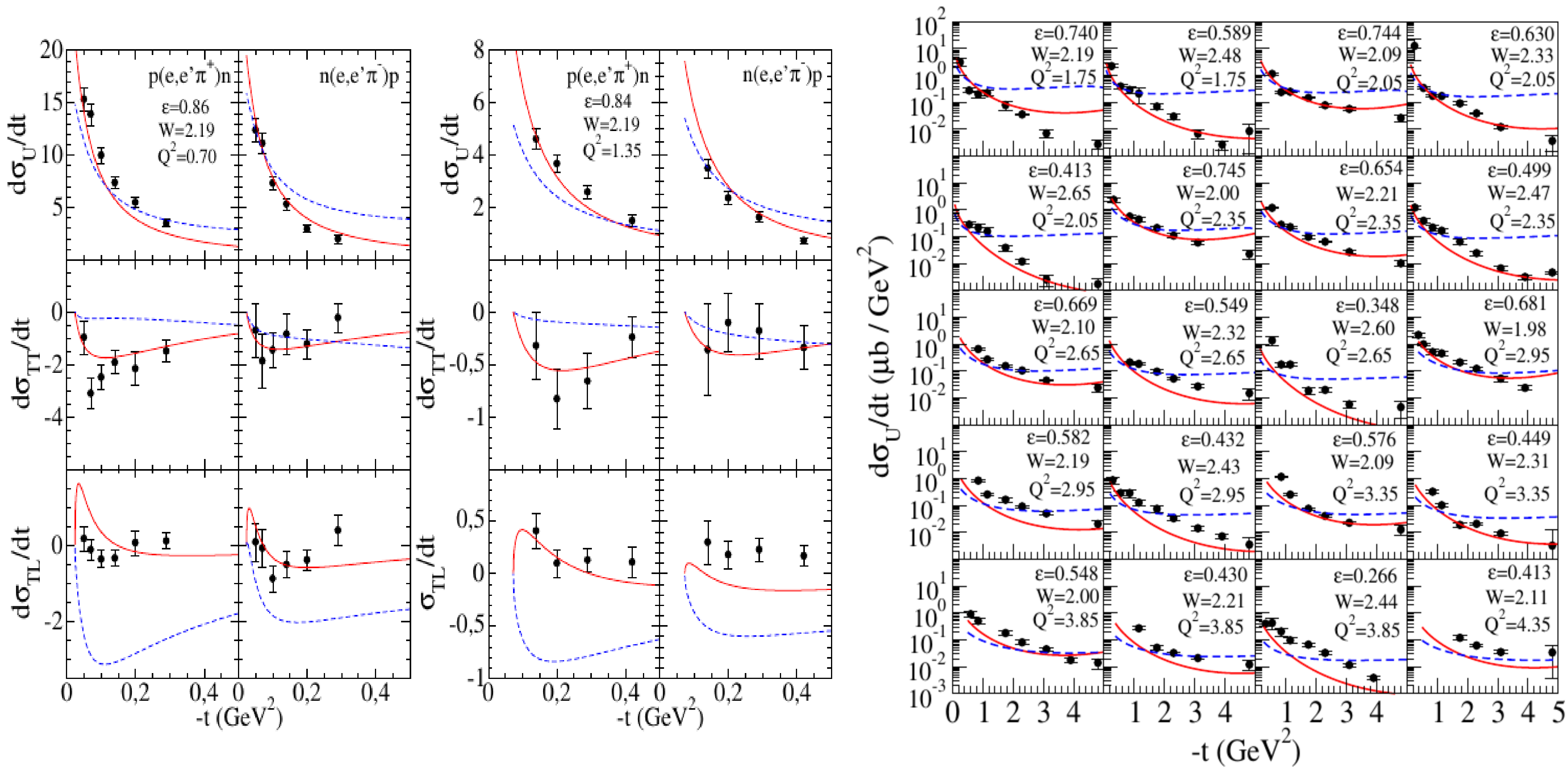

Figure: High-energy model (red lines), low-energy model (blue lines) and **electron-induced single-pion production** data.

High-energy model

Regge approach for the axial amplitudes.

We need meson exchange diagrams to apply the reggeization procedure of the current.

Effective rho-exchange diagrams. This allows us to consider the rho-exchange as the main Regge trajectory in the axial current.

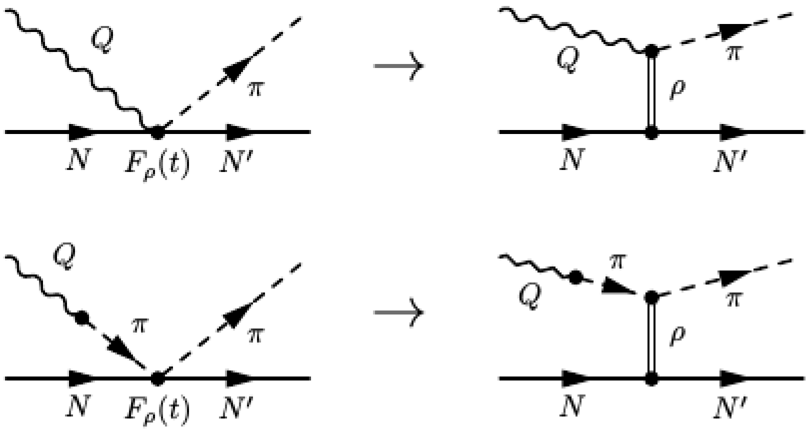

$$\mathcal{O}^{\mu}_{CT\rho} = i\mathcal{I}\,\frac{m_\rho^2}{m_\rho^2 - t} F_{A\rho\pi}(Q^2)\frac{1}{\sqrt{2}f_\pi} \times \left(\gamma^\mu + i\frac{\kappa_\rho}{2M}\sigma^{\mu\nu}K_{t,\nu}\right) .$$

We consider $\kappa_\rho = 0$ so that the low-energy model amplitude is recovered.

The propagator of the rho is replaced by the Regge trajectory of the **rho family**:

$$\mathcal{P}_\rho(t,s) = -\alpha'_\rho \varphi_\rho(t)\Gamma[1-\alpha_\rho(t)](\alpha'_\rho s)^{\alpha_\rho(t)-1}$$

High-energy model

Regge approach for the axial amplitudes.

We need meson exchange diagrams to apply the reggeization procedure of the current.

Effective rho-exchange diagrams. This allows us to consider the rho-exchange as the main Regge trajectory in the axial current.

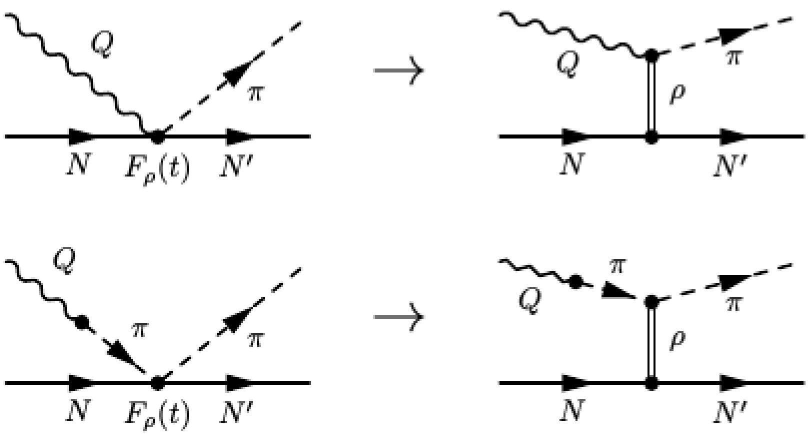

$$\mathcal{O}^{\mu}_{CT\rho} = i\mathcal{I}\,\frac{m_\rho^2}{m_\rho^2 - t} F_{A\rho\pi}(Q^2)\,\frac{1}{\sqrt{2}f_\pi} \times \left(\gamma^\mu + i\frac{\kappa_\rho}{2M}\sigma^{\mu\nu}K_{t,\nu}\right).$$

We consider $\kappa_\rho = 0$ so that the low-energy model amplitude is recovered.

+ 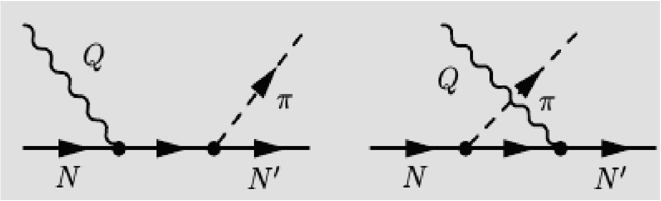 ?

High-energy model

"Reggeizing" the ChPT background:

$$\mathcal{O}^{\mu}_{ReChi,V} = \mathcal{O}^{\mu}_{ChPT,V}\,\underbrace{\mathcal{P}_{\pi}(t,s)(t-m_{\pi}^{2})}$$

high-energy model: ReChi (from Reggeized ChPT background)

low-energy model (only the ChPT background)

The pion propagator is replaced by the **Regge propagator** of the pion trajectory

$$\mathcal{O}^{\mu}_{ReChi,A} = \mathcal{O}^{\mu}_{ChPT,A}\,\mathcal{P}_{\rho}(t,s)(t-m_{\rho}^{2})$$

High-energy model: results for neutrinos

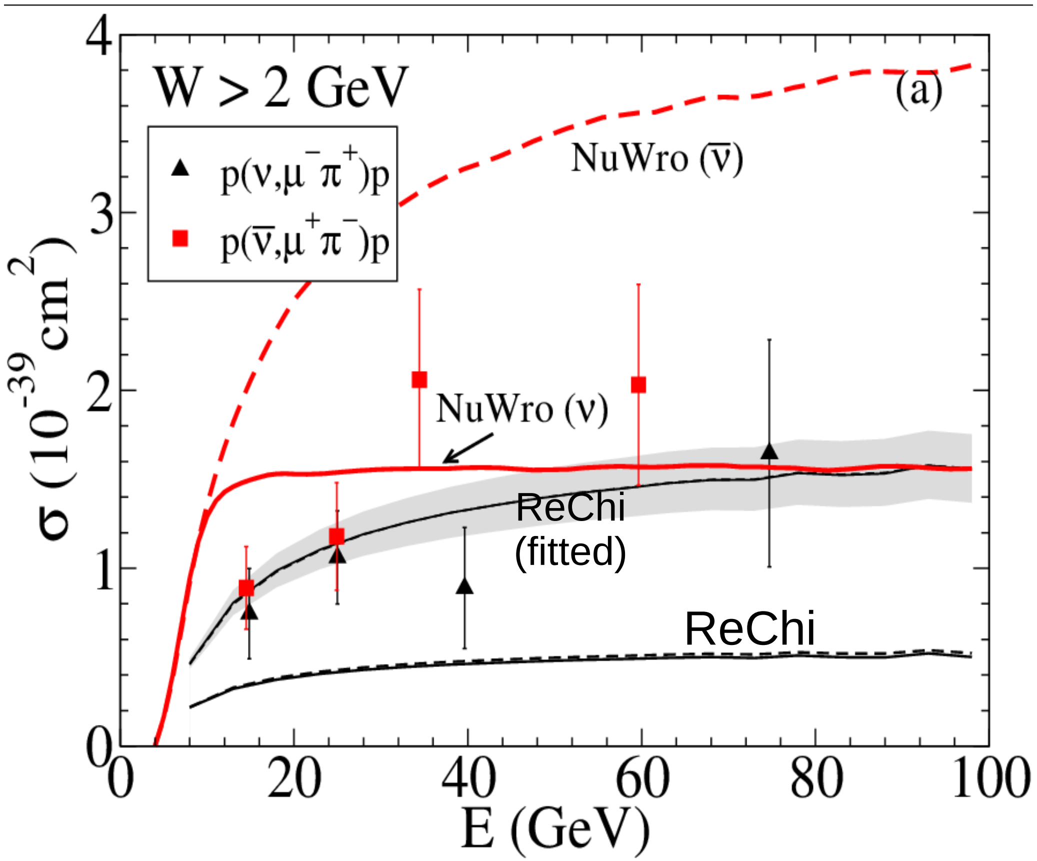

Figure: ReChi model and NuWro predictions are compared with high energy cross section data for neutrino and antineutrino reactions (Note the high energy cut W>2 GeV !!). Data from Allen et al. NPB264, 221 (1986).

NuWro: Based on DIS formalism and PYTHIA for hadronization.

Antineutrino cross section is ~2 the neutrino one:

$$\bar{\nu} + \overbrace{uud}^{p} \rightarrow \mu^{+} + \overbrace{\bar{u}d}^{\pi^{-}} + uud\,,$$
$$\nu + uud \rightarrow \mu^{-} + \underbrace{u\bar{d}}_{\pi^{+}} + uud\,.$$

ReChi model: One free parameter in the boson-nucleon-nucleon vertex

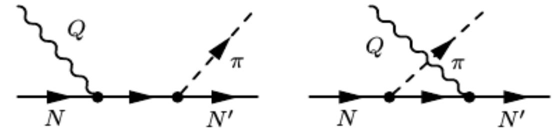

$$G_A[Q^2, s(u)] = g_A \left(1 + \frac{Q^2}{\Lambda_{Apn^*}[s(u)]^2}\right)^{-2}$$

$$\Lambda_{Anp^*}(s) = \Lambda_{Apn} + (\Lambda_\infty^A - \Lambda_{Apn})\left(1 - \frac{M^2}{s}\right)$$

$\Lambda_\infty^A = (7.20 \pm {}^{2.09}_{1.32})$ GeV !!!

Low Energy Model

+

High Energy Model

= Hybrid Model

Hybrid model

1) Regularizing the behavior of resonances (u- and s-channel contributions): we multiply the resonance amplitude by a dipole-Gaussian form factor

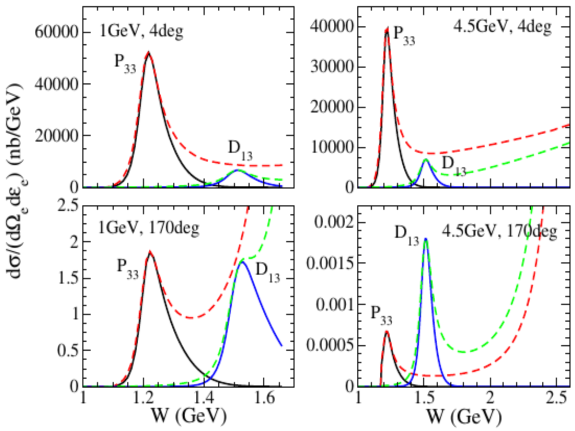

$$F(s,u) = F(s) + F(u) - F(s)F(u)$$

$$F(s) = \exp\left(\frac{-(s-M_R^2)^2}{\lambda_R^4}\right) \frac{\lambda_R^4}{(s-M_R^2)^2 + \lambda_R^4}$$

2) Gradually replacing the ChPT background by the High-energy (ReChi) model: we use a phenomenological transition function

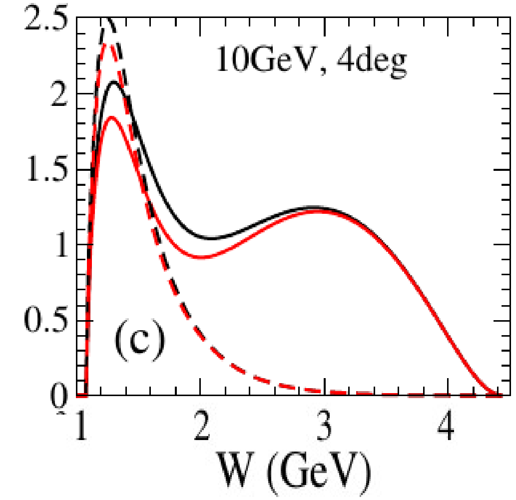

$$\widetilde{\mathcal{O}} = \cos^2\phi(W)\mathcal{O}_{ChPT} + \sin^2\phi(W)\mathcal{O}_{ReChi}$$

$$\phi(W) = \frac{\pi}{2}\left(1 - \frac{1}{1+\exp\left[\frac{W-W_0}{L}\right]}\right) , \quad W_0 = 1.7 \text{ GeV}, \quad L = 100 \text{ MeV}$$

Hybrid model: results

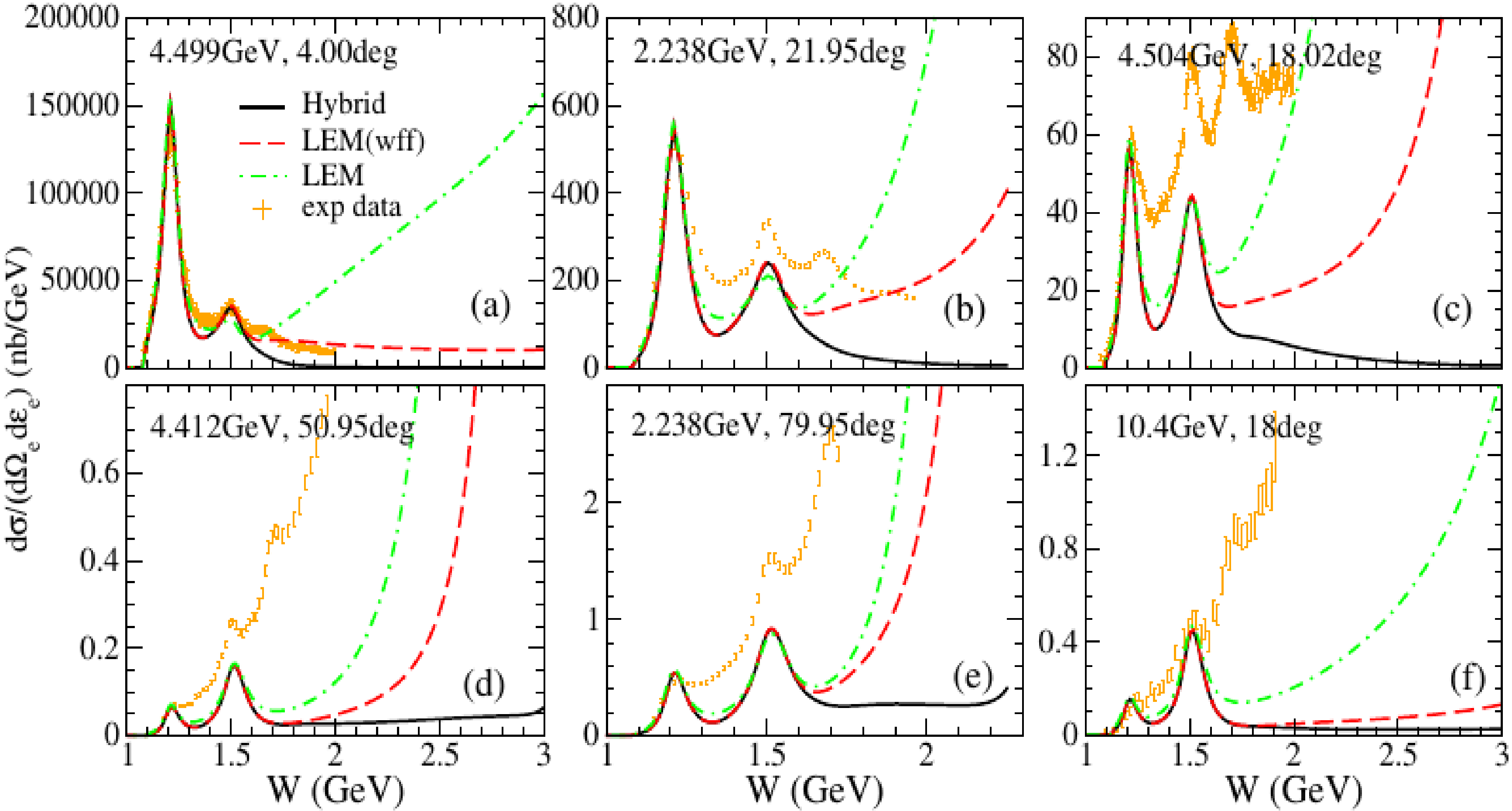

Hybrid model: results

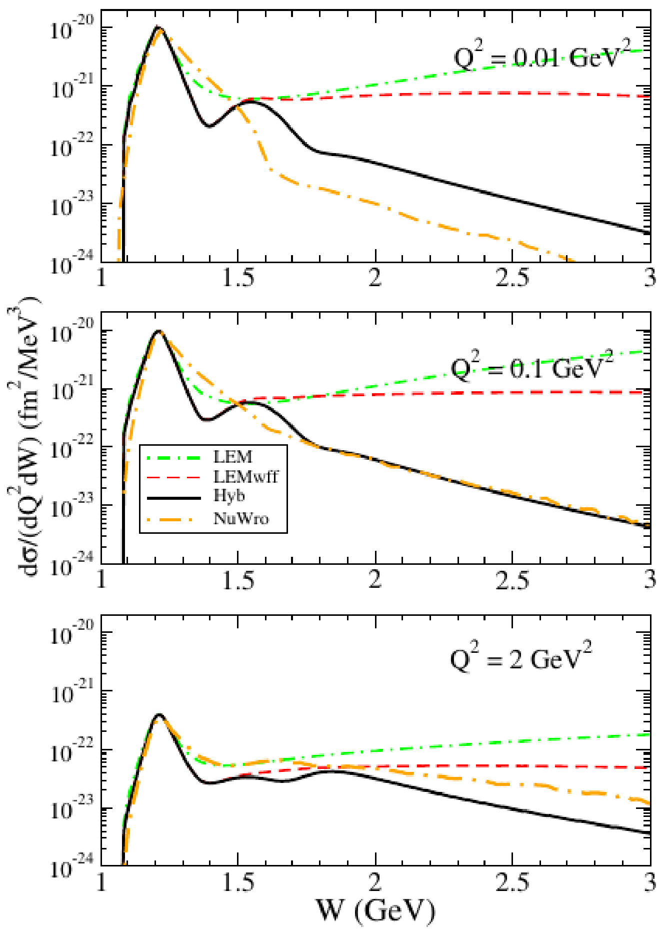

FIG. 21. (Color online) Different model predictions for the differential cross section $d\sigma/(dQ^2dW)$, for the channel $p(\nu_\mu, \mu^- \pi^+)p$. The incoming neutrino energy is fixed to $E_\nu = 10$ GeV.

Hybrid model: results

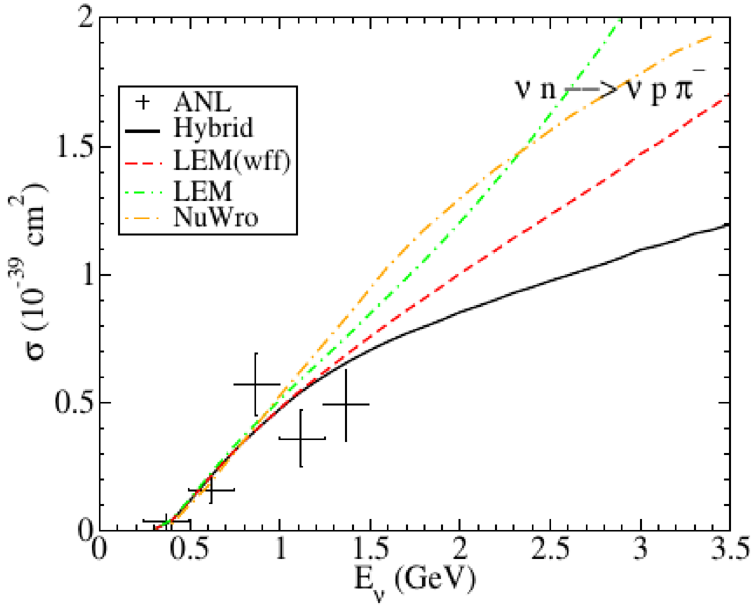

Figure: Predictions for the WNC.

Hybrid model: results

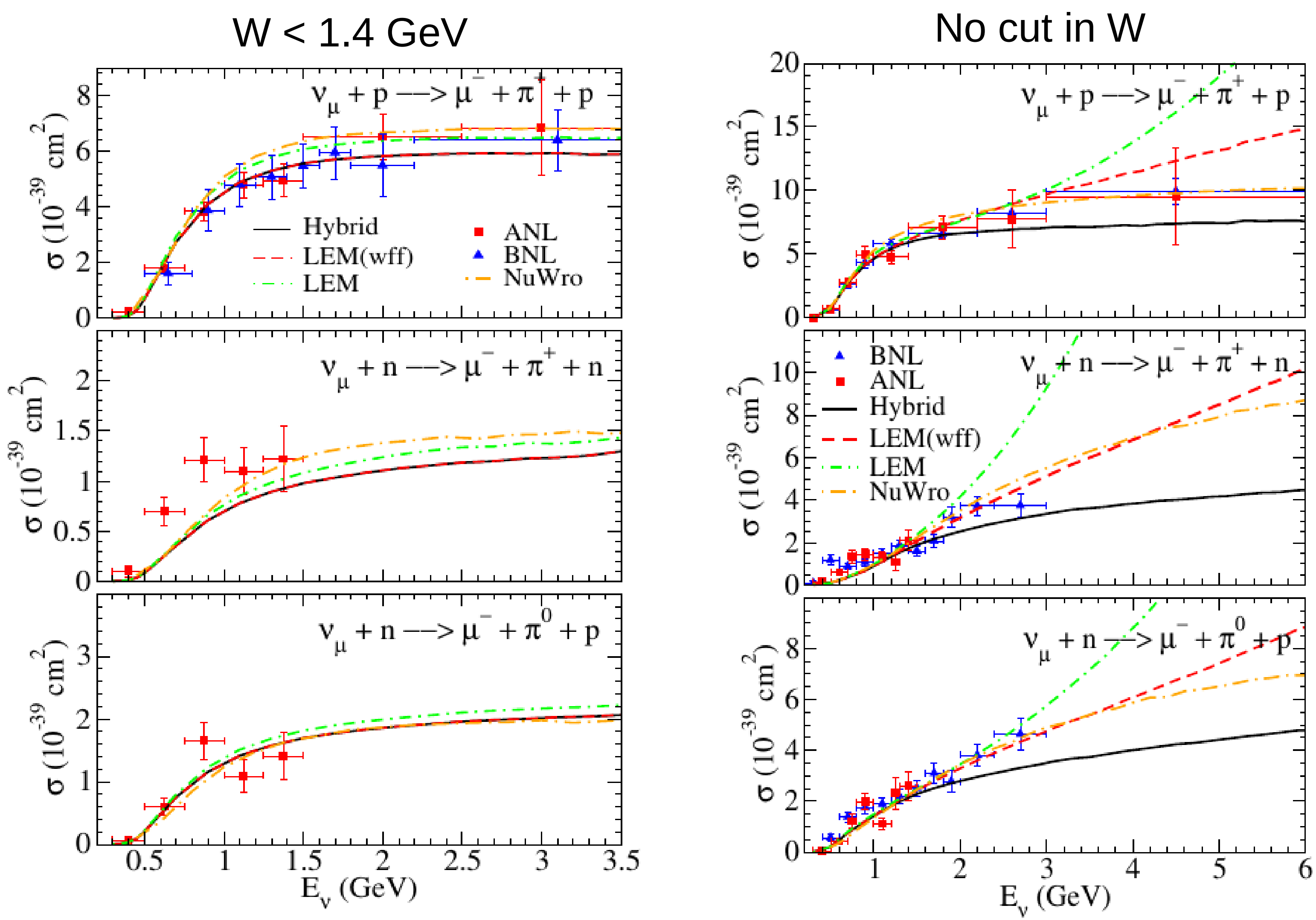

More details in ...

PHYSICAL REVIEW D **95,** 113007 (2017)

Electroweak single-pion production off the nucleon: From threshold to high invariant masses

R. González-Jiménez,[1,*] N. Jachowicz,[1] K. Niewczas,[1,2] J. Nys,[1] V. Pandey,[3] T. Van Cuyck,[1] and N. Van Dessel[1]

[1]*Department of Physics and Astronomy, Ghent University, Proeftuinstraat 86, B-9000 Gent, Belgium*
[2]*Institute of Theoretical Physics, University of Wrocław, Plac Maxa Borna 9, 50-204 Wrocław, Poland*
[3]*Center for Neutrino Physics, Virginia Tech, Blacksburg, Virginia 24061, USA*

(Received 15 December 2016; published 30 June 2017)

III Nuclear effects

Electroweak one-pion production on nuclei

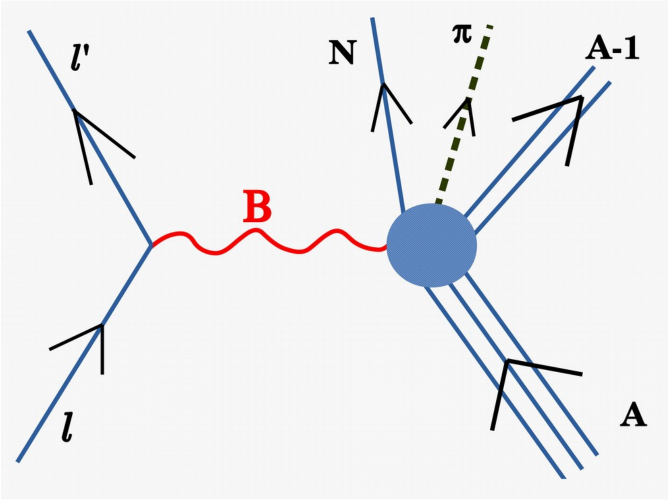

PRD 97, 013004 (2018), PRD 97, 093008 (2018)

$$\frac{d^9\sigma}{d\varepsilon_f d\Omega_f \, dE_\pi d\Omega_\pi \, d\Omega_N \, dE_m} \propto \ell_{\mu\nu} H^{\mu\nu}$$

$$\begin{aligned} \ell_{\mu\nu} &= \overline{\sum} (j_\mu)^* j_\nu \\ H^{\mu\nu} &= \overline{\sum} (J^\mu)^* J^\nu \end{aligned}$$

$$\begin{aligned} j_\mu &= j_\mu(\varepsilon_i, q, \omega) \,, \\ J^\mu &= J^\mu(q, \omega, E_\pi, \theta_\pi, \phi_\pi, \theta_N, \phi_N, E_m) \end{aligned}$$

$$\frac{d^9\sigma}{d\varepsilon_f d\Omega_f \, dE_\pi d\Omega_\pi \, d\Omega_N \, dE_m} \propto \ell_{\mu\nu} H^{\mu\nu}$$

$$\ell_{\mu\nu} = \overline{\sum} (j_\mu)^* j \ldots$$

$$H^{\mu\nu} = \overline{\sum} (\ldots$$

8 indep. variables.

$$j_\mu = j_\mu(\varepsilon_i, q, \omega) ,$$

$$J^\mu = J^\mu(q, \omega, E_\pi, \theta_\pi, \phi_\pi, \theta_N, \phi_N, E_m)$$

Relativistic mean field model

Relativistic Impulse Approximation

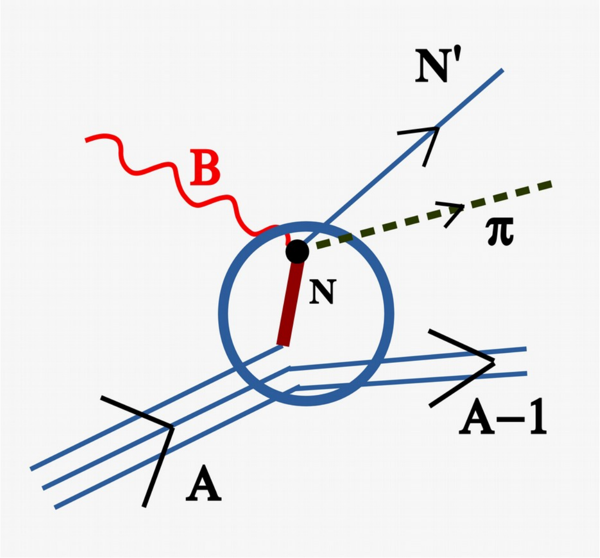

$$J^{\mu}_{had} = \sum_{i}^{A} \int d\mathbf{r}\, \overline{\Psi}_F(\mathbf{r})\, \phi^*(\mathbf{r}) \hat{\mathcal{O}}^{\mu}_{one\text{-}body}(\mathbf{r})\, \Psi_B(\mathbf{r})\; e^{i\mathbf{q}\cdot\mathbf{r}}$$

Relativistic mean-field wave functions

$$\frac{d^9\sigma}{d\varepsilon_f d\cos\theta_f d\phi_f\, dE_\pi d\cos\theta_\pi d\phi_\pi\, d\cos\theta_N d\phi_N\, dE_m}$$

Easy and fast...

π

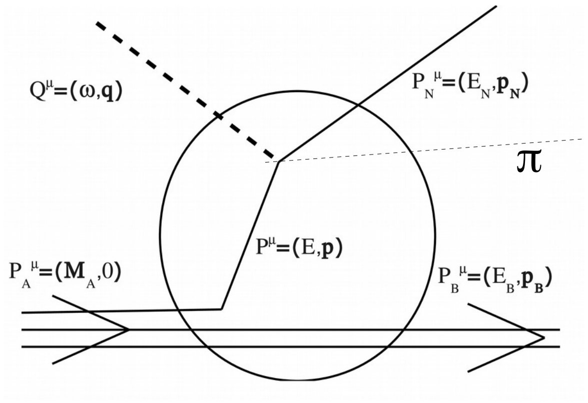

RPWIA: Scattered nucleon wf is described as a Dirac plane wave.

Final Nucleon: Plane wave

Pion:Plane wave

$$J^{\mu}_{had} = \sum_{i}^{A} \int d\mathbf{r}\, \overline{\Psi}_F(\mathbf{r})\, \phi^*(\mathbf{r}) \hat{O}^{\mu}_{one\text{-}body}(\mathbf{r})\, \Psi_B(\mathbf{r})\, e^{i\mathbf{q}\cdot\mathbf{r}}$$

relativistic mean-field wave function

Easy and fast...

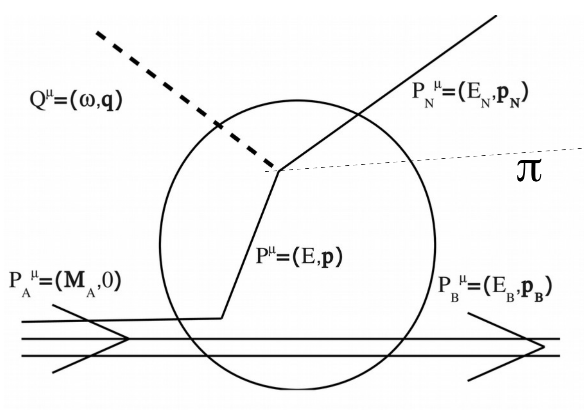

RPWIA: Scattered nucleon wf is described as a Dirac plane wave.

Complex and heavy...

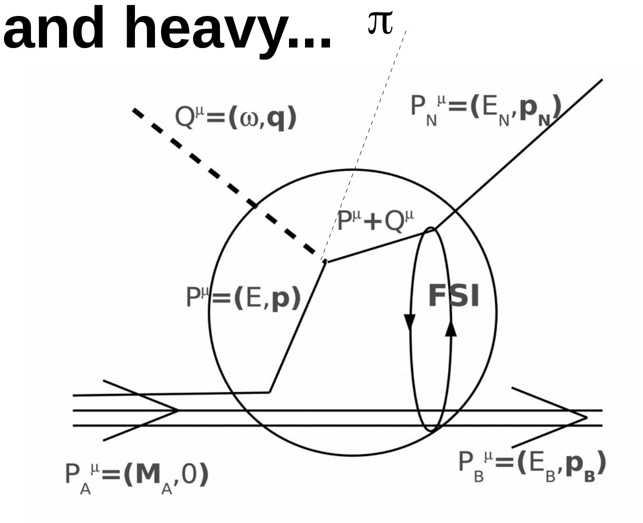

RMF-FSI: Scattered nucleon wf is solution of Dirac eq. in presence of the same potentials used to describe the bound nucleon wf.

Pion:Plane wave

$$J^\mu_{had} = \sum_i^A \int d\mathbf{r}\, \overline{\Psi}_F(\mathbf{r})\, \phi^*(\mathbf{r}) \hat{O}^\mu_{one\text{-}body}(\mathbf{r})\, \Psi_B(\mathbf{r})\, e^{i\mathbf{q}\cdot\mathbf{r}}$$

relativistic mean-field wave functions

Nuclear effects in electron- and neutrino-nucleus scattering within a relativistic quantum mechanical framework

R. González-Jiménez,[1] A. Nikolakopoulos,[2] N. Jachowicz,[2] and J.M. Udías[1]

http://arxiv.org/abs/1904.10696v1

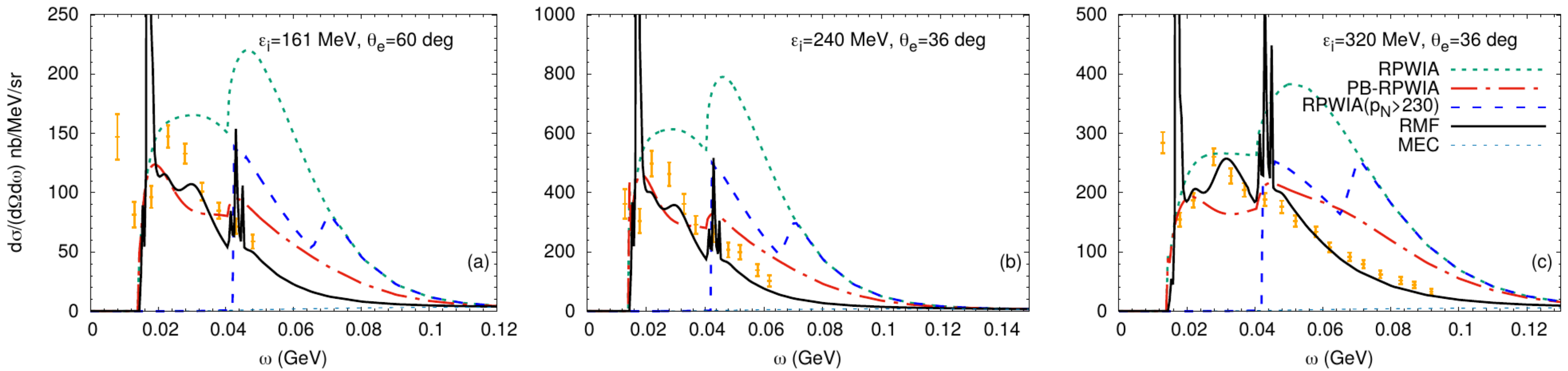

FIG. 4: QE predictions for the process $^{12}C(e,e')$ with the RPWIA, PB-RPWIA, RPWIA($p_N > 230$), and RMF models. The MEC contribution [55] is shown separately. Although it is negligible at these kinematics, it has been added to the QE response. ε_i is the incident electron energy and θ_e the scattering angle. Data taken from [57].

Orthogonality: Pauli blocking

Partial wave expansion of a relativistic plane wave:

$$\Psi_{PW}(\mathbf{r},\mathbf{p},m_s) = 4\pi\sqrt{\frac{E+M}{2EV}}\sum_{\kappa=-\infty}^{+\infty}\sum_{m_j=-j}^{+j} i^{\ell}\langle\ell(m_j-m_s),\frac{1}{2}m_s|jm_j\rangle[Y_\ell^{m_\ell}(\Omega_{\mathbf{p}})]^* \times \begin{pmatrix} j_\ell(pr)\phi_\kappa^{m_j}(\Omega_{\mathbf{r}}) \\ i\frac{|\kappa|}{\kappa}j_{\bar{\ell}}(pr)\phi_{-\kappa}^{m_j}(\Omega_{\mathbf{r}}) \end{pmatrix}.$$

The **orthogonalized** final nucleon wave function (Pauli blocked) is built by subtracting to the plane wave the partial waves that overlap with the initial state nucleus:

$$|\Psi^{s_N}(\mathbf{p}_N)\rangle = |\psi_{pw}^{s_N}(\mathbf{p}_N)\rangle - \sum_{\kappa,m_j}[C_\kappa^{m_j,s_N}(\mathbf{p}_N)]^\dagger\,|\psi_\kappa^{m_j}\rangle$$

$$C_\kappa^{m_j,s_N}(\mathbf{p}_N) \equiv \langle\psi_{pw}^{s_N}(\mathbf{p}_N)|\psi_\kappa^{m_j}\rangle$$

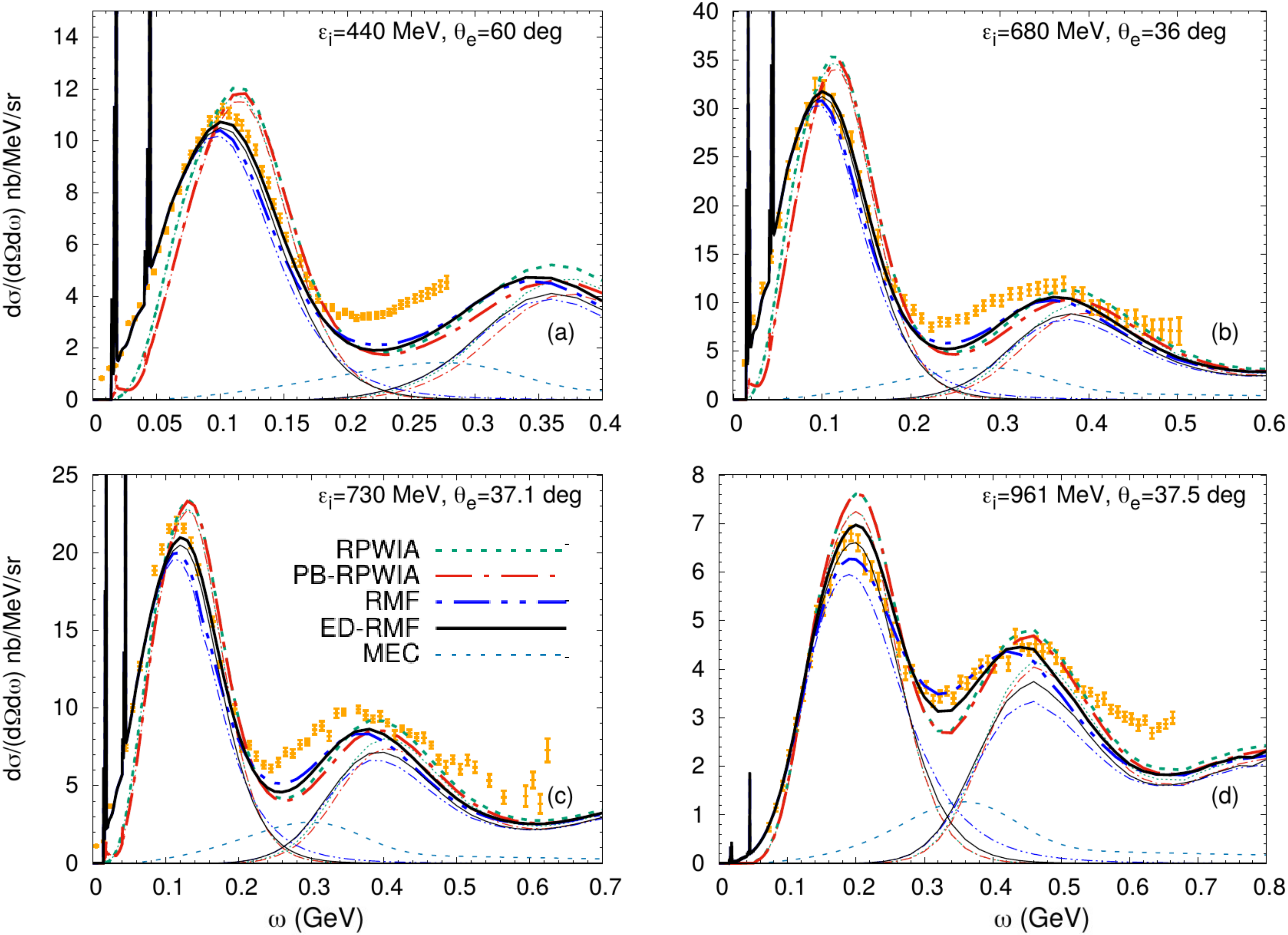

FIG. 5: QE and SPP for the process $^{12}C(e,e')$ with the RPWIA, PB-RPWIA, RMF and ED-RMF models. MEC was taken from Ref. [55]. The QE+MEC+SPP cross sections are represented by the thicker lines, while the QE and SPP cross sections correspond to the thinner lines. Data from [57].

Energy-dependent relativistic mean-field (**ED-RMF**) model

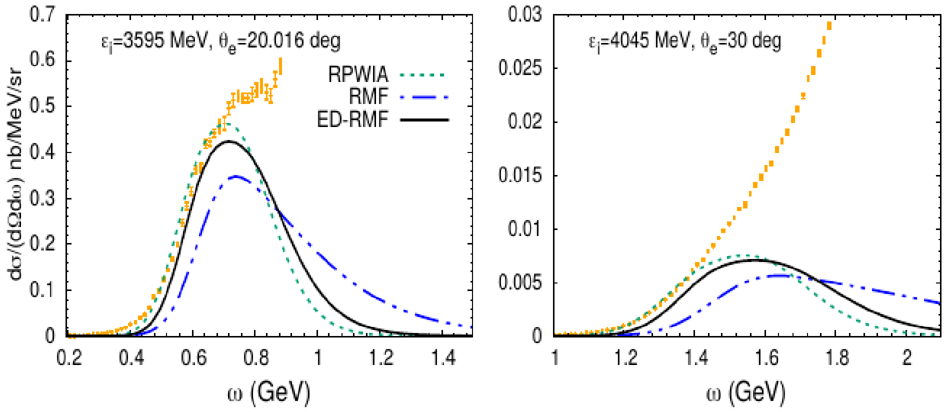

FIG. 6: QE contribution computed with RPWIA, RMF and ED-RMF models. Data taken from [57].

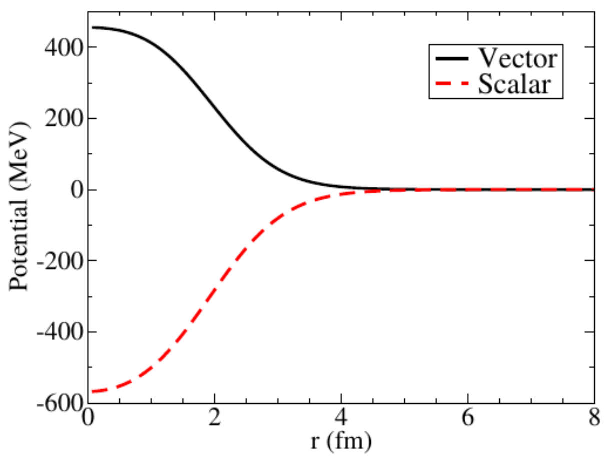

FIG. 2: RMF vector and scalar potentials as a function of the position r in the ^{12}C nucleus.

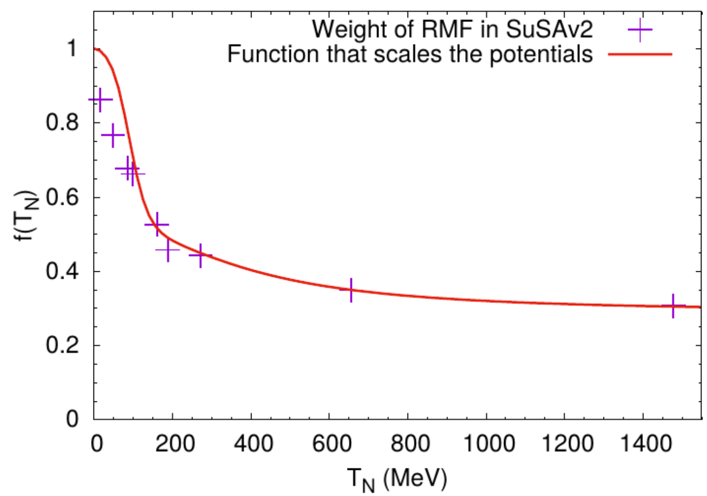

FIG. 3: Function that scales the RMF potentials.

The **ED-RMF** model is essentially equivalent to use energy-dependent optical potentials, that were fitted to reproduce elastic proton-nucleus scattering…

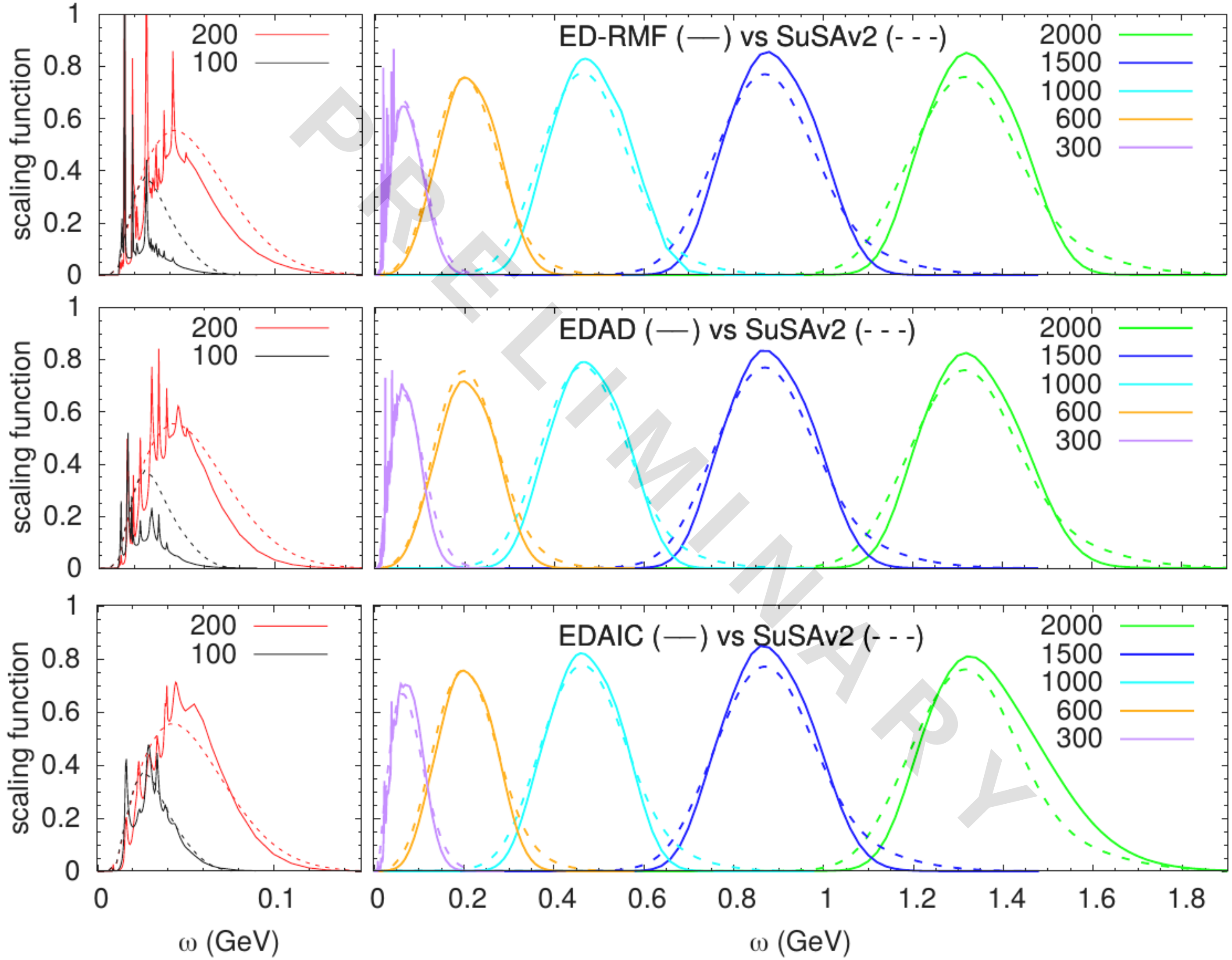

… and these are surprisingly similar to SuSAv2 approach. What a coincidence!

SuSAv2 vs ED-RMF vs JLab data

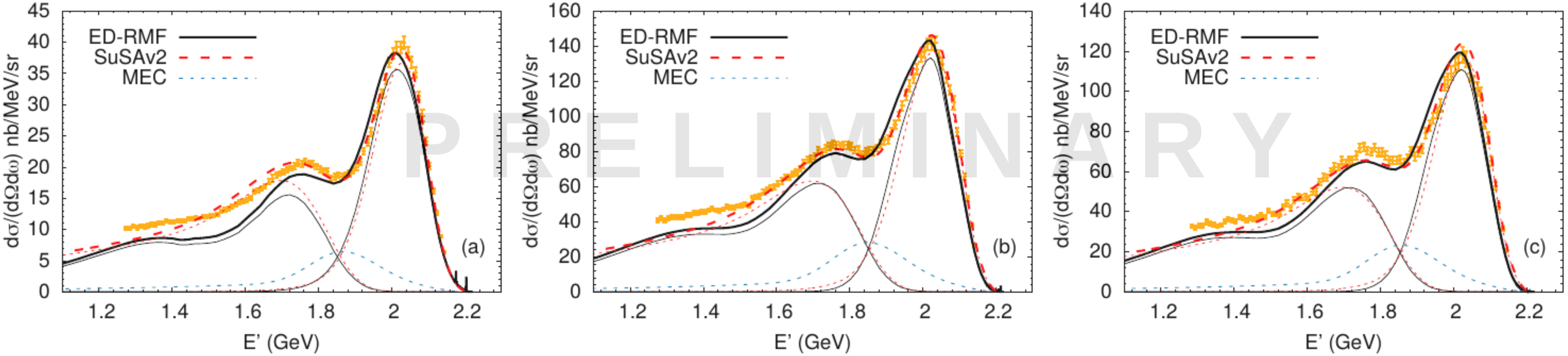

Fig.: SuSAv2 and ED-RMF results compared to recent (e,e') JLab data for 12C, 48Ti, and 40Ar. Incident energy 2222 MeV, scattering angle 15.541 deg.

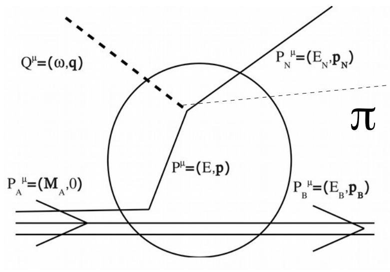

RPWIA: Scattered nucleon and pion wf is described as a plane waves.

MiniBooNE neutrino CC 1pion+

MINERvA antineutrino CC 1pion0.

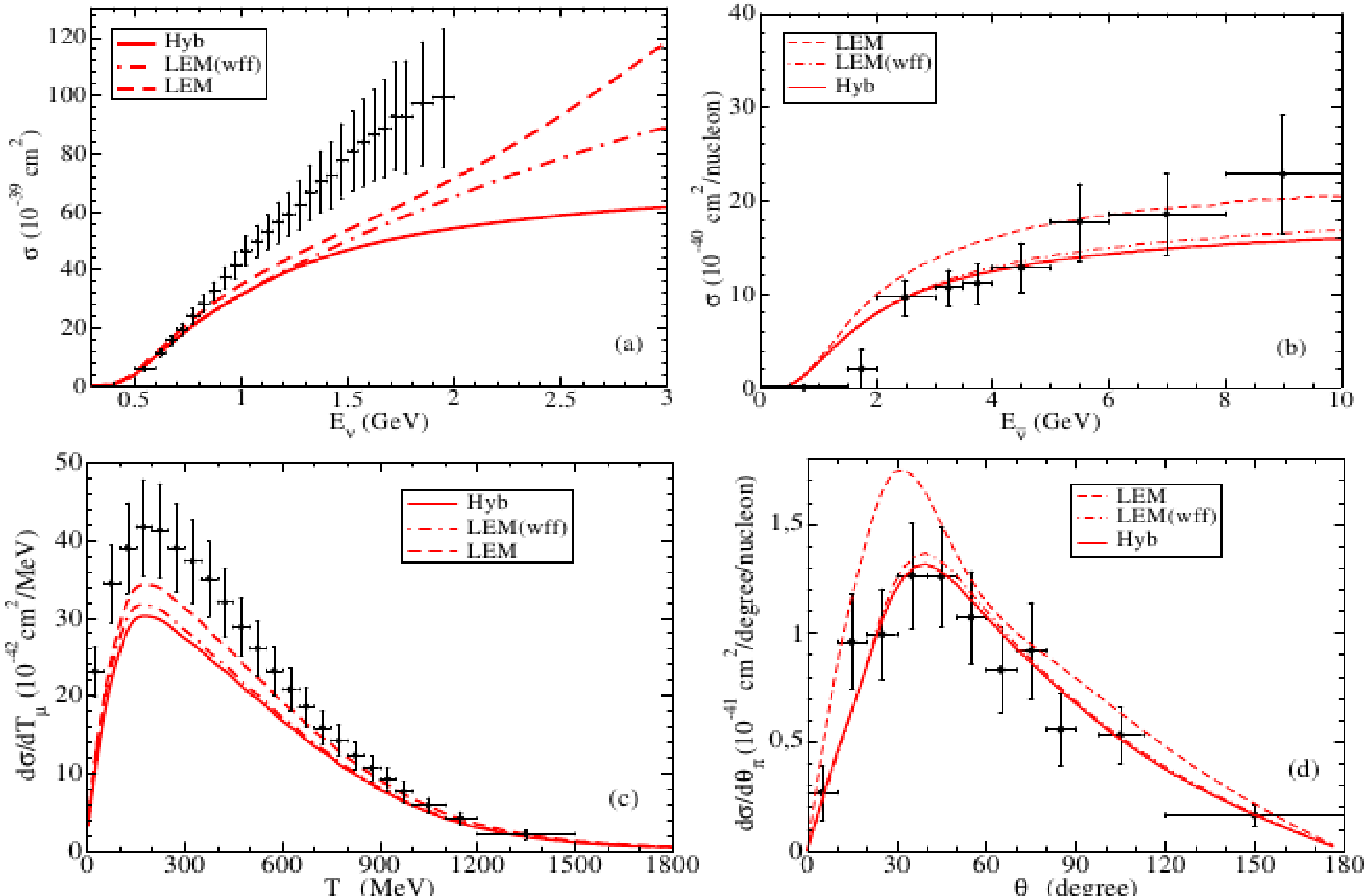

PRD 97, 013004 (2018)

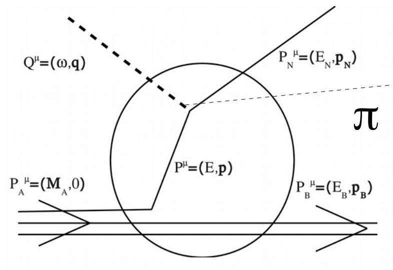

RPWIA: Scattered nucleon and pion wf is described as a plane waves.

MiniBooNE neutrino CC 1pion+.

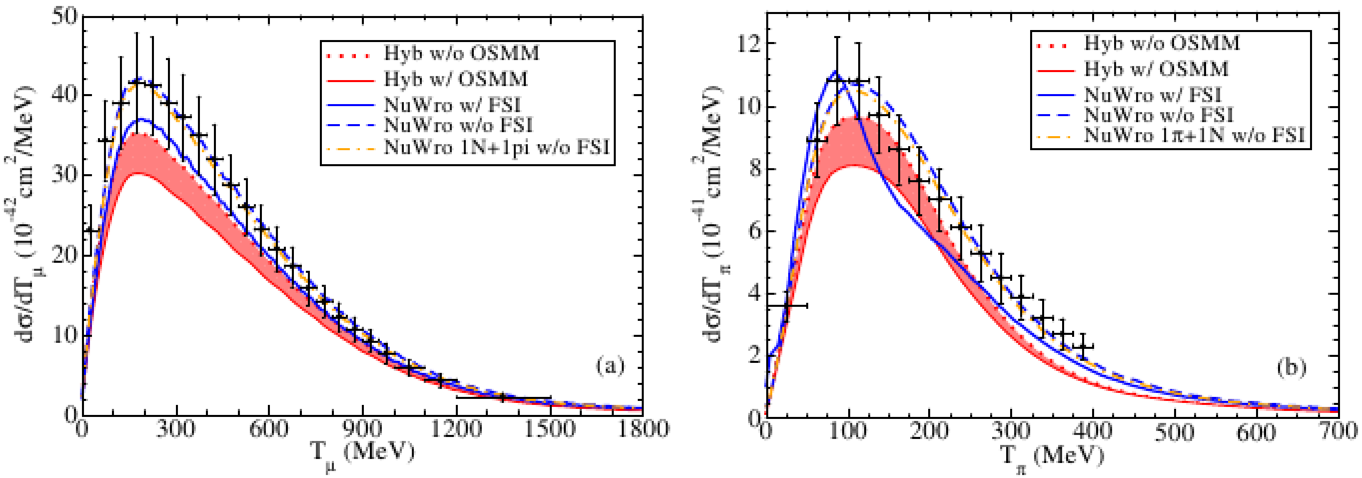

MINERvA neutrino CC 1pion+.

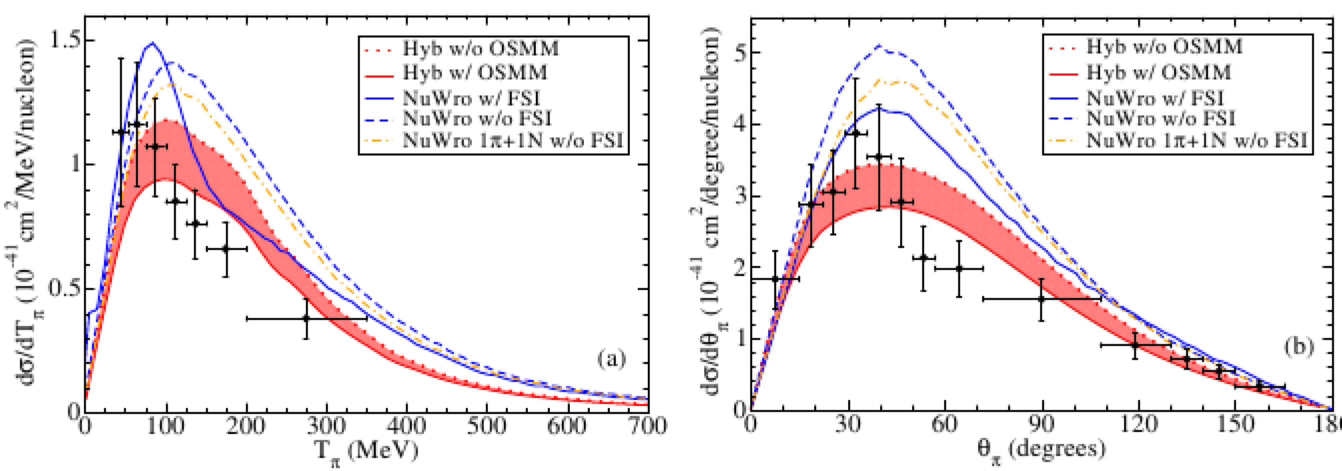

PRD 97, 013004 (2018)

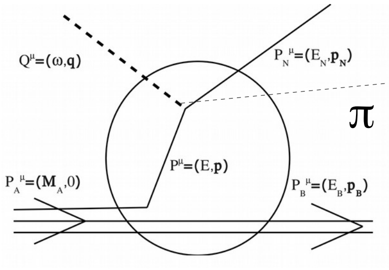

RPWIA: Scattered nucleon and pion wf is described as a plane waves.

MiniBooNE neutrino CC 1pion0.

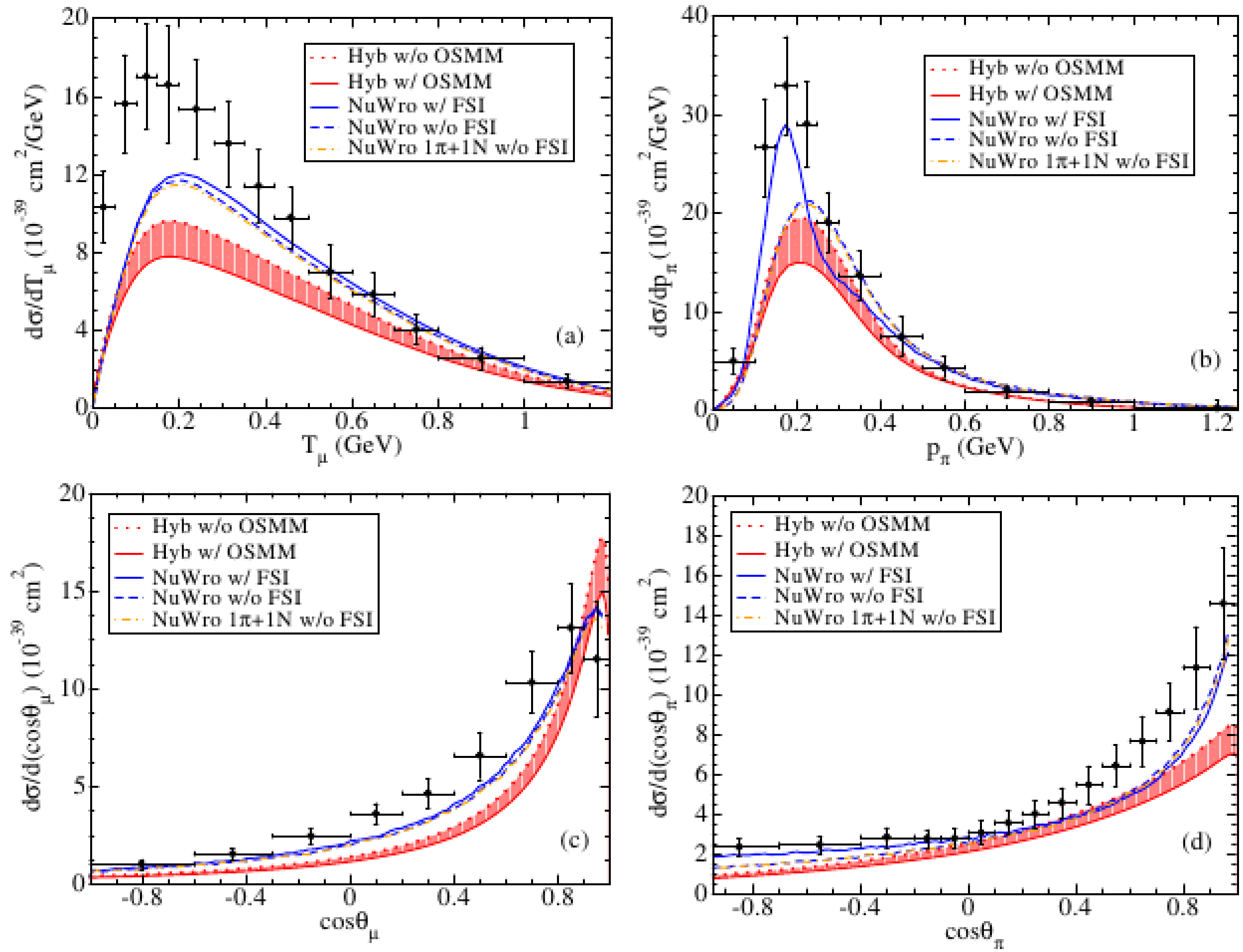

PRD 97, 013004 (2018)

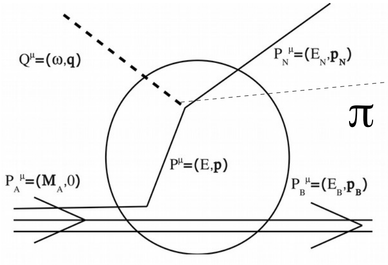

RPWIA: Scattered nucleon and pion wf is described as a plane waves.

MINERvA neutrino CC 1pion0.

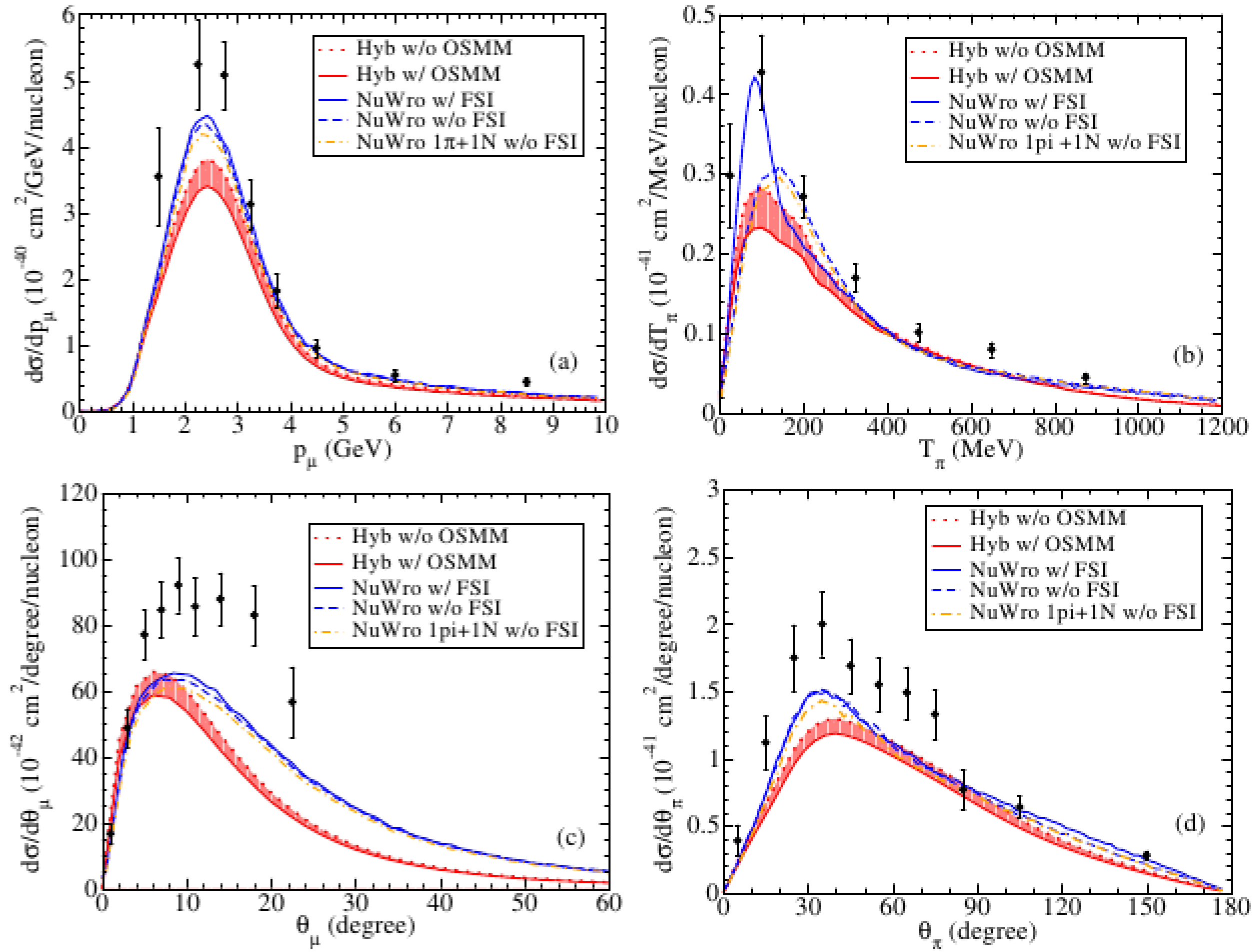

PRD 97, 013004 (2018)

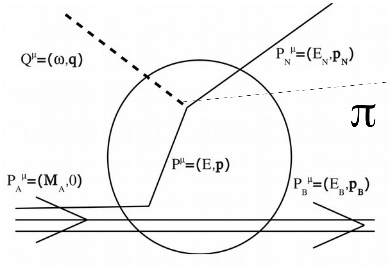

RPWIA: Scattered nucleon and pion wf is described as a plane waves.

MINERvA antineutrino CC 1pion0.

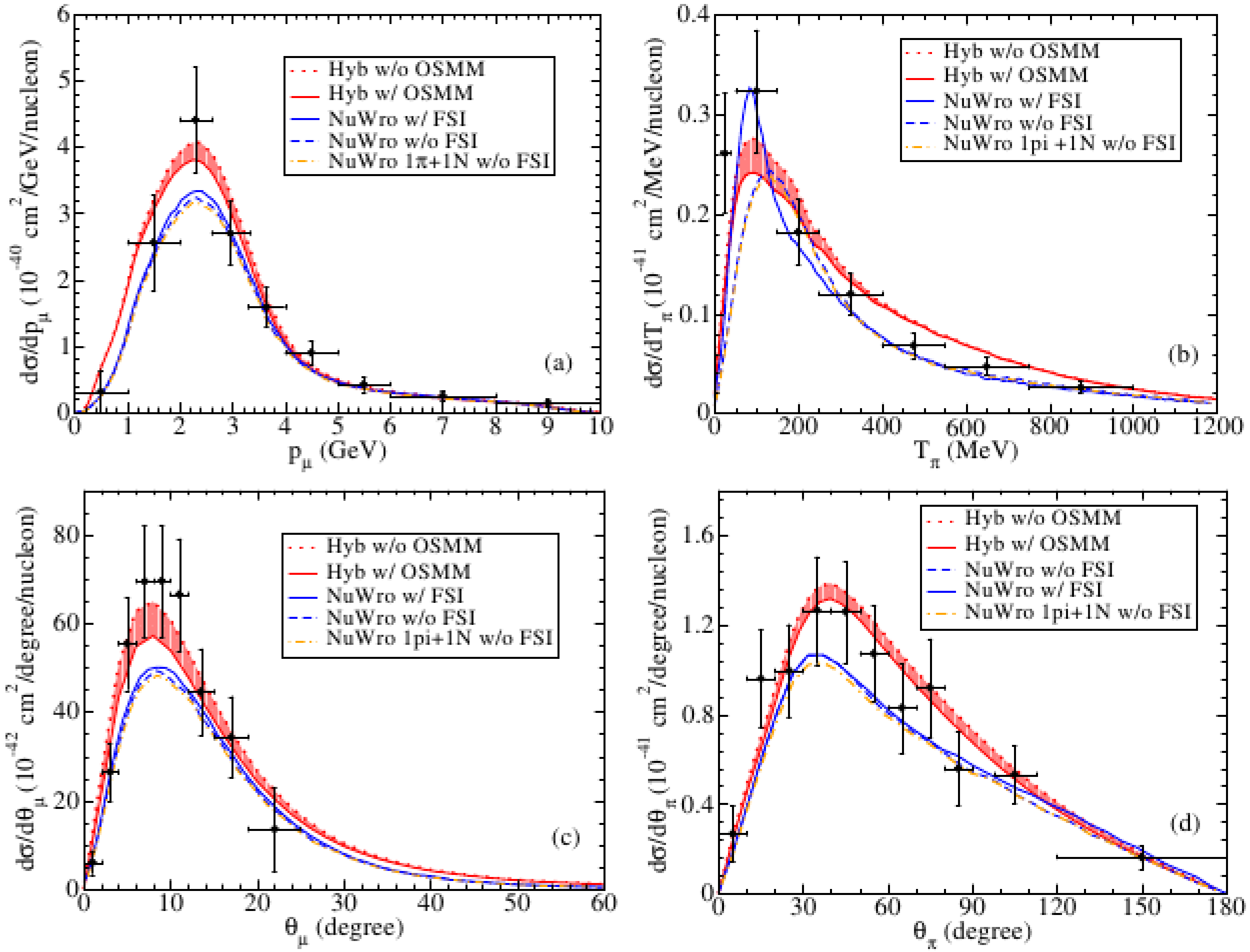

PRD 97, 013004 (2018)

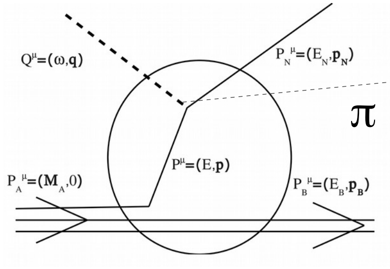

RPWIA: Scattered nucleon and pion wf is described as a plane waves.

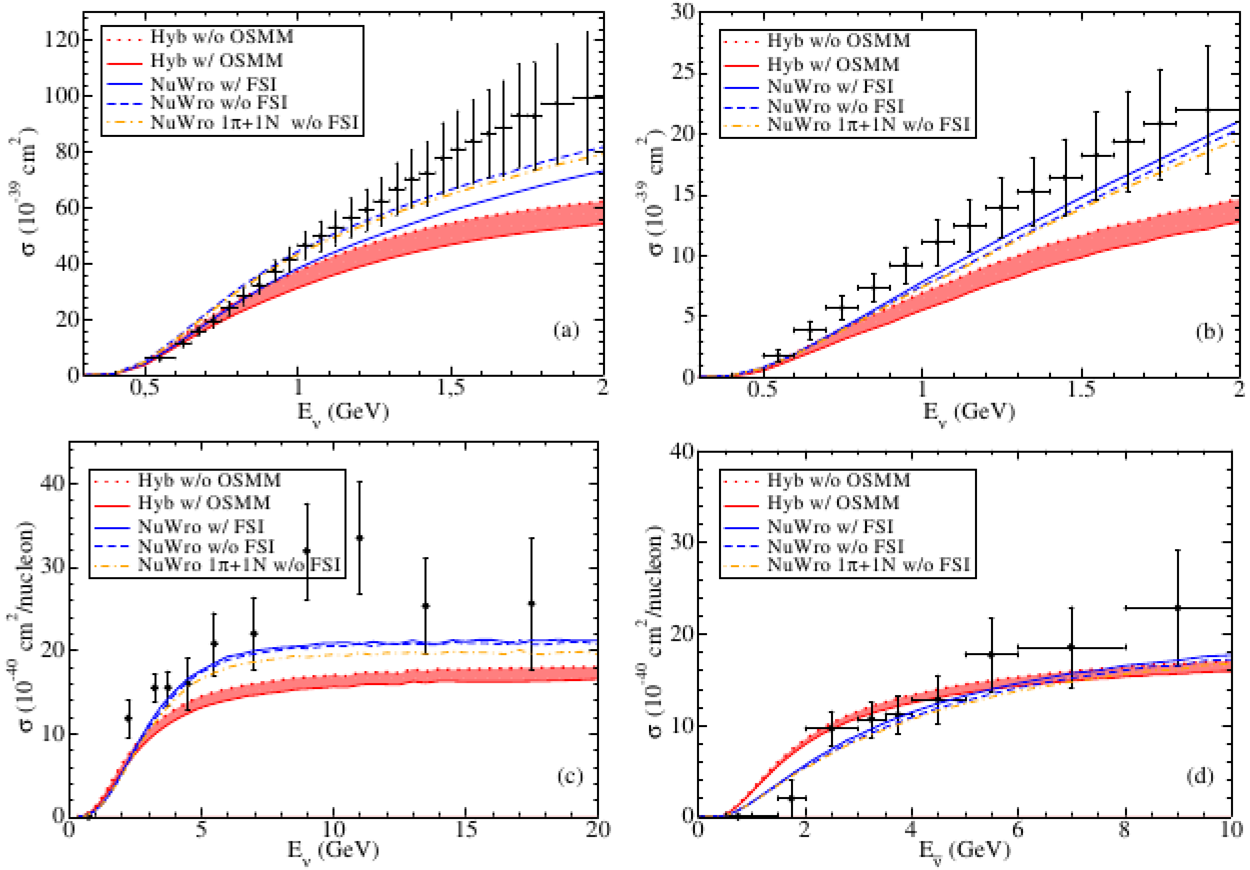

FIG. 10: Total cross section for the reactions (a) MiniBooNE νCC $1\pi^+$ [4], (b) MiniBooNE νCC $1\pi^0$ [62], (c) MINERvA νCC $1\pi^0$ [7], and (d) MINERvA $\bar{\nu}$CC $1\pi^0$ [6]. Labels as in Fig. 5

PRD 97, 013004 (2018)

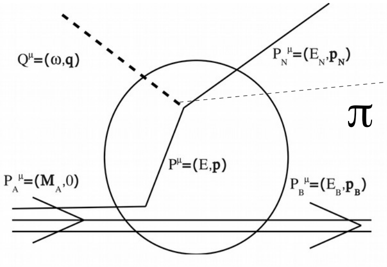

RPWIA: Scattered nucleon and pion wf is described as a plane waves.

T2K CC 1pion+

PRD 97, 093008 (2018)

LEM vs Hybrid

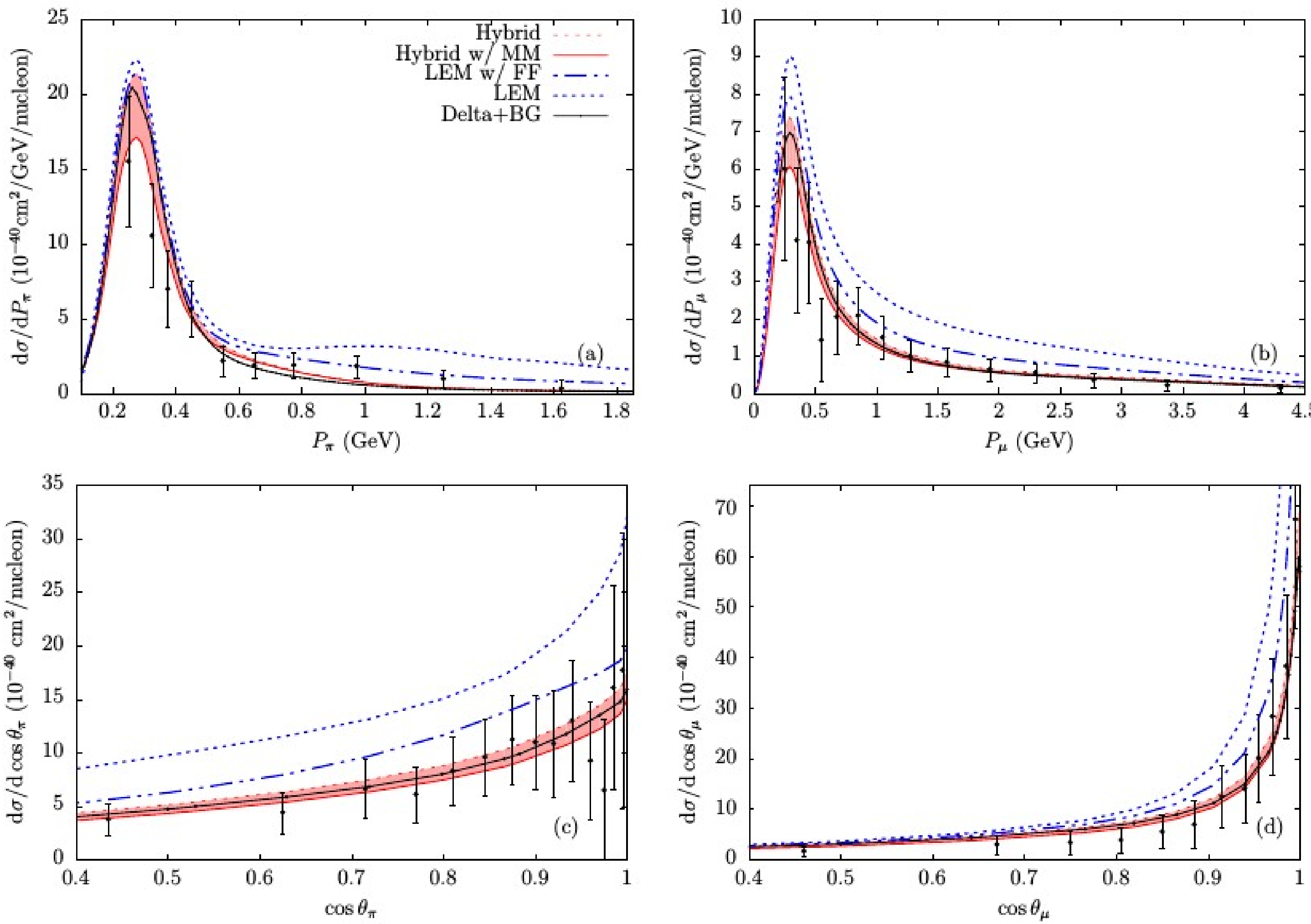

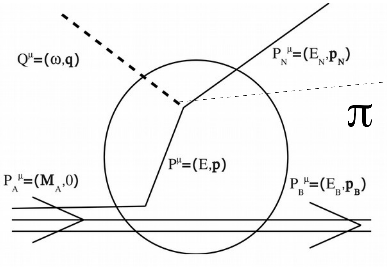

T2K CC 1pion+

PRD 97, 093008 (2018)

NuWro vs Hybrid: pion FSI effects

RPWIA: Scattered nucleon and pion wf is described as a plane waves.

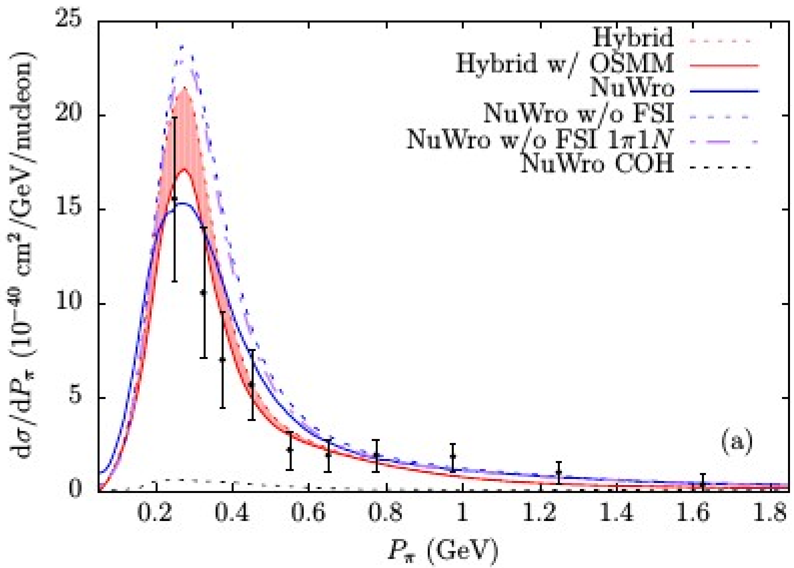

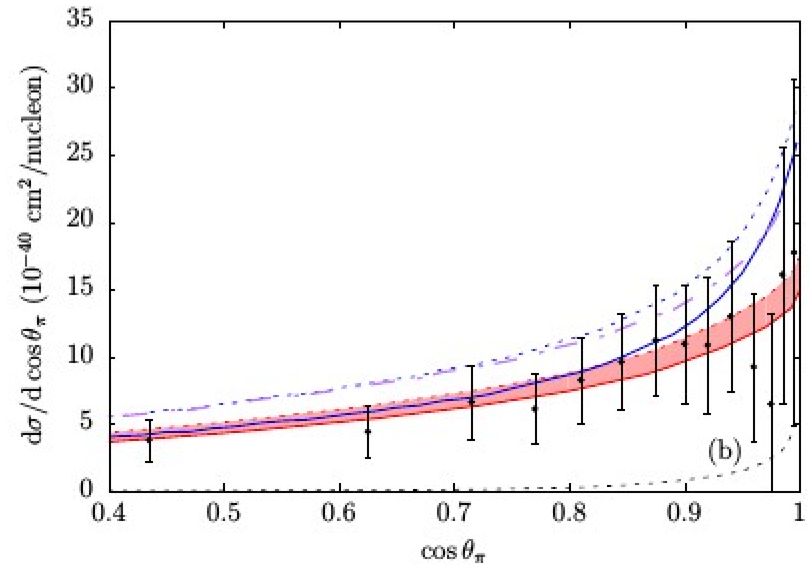

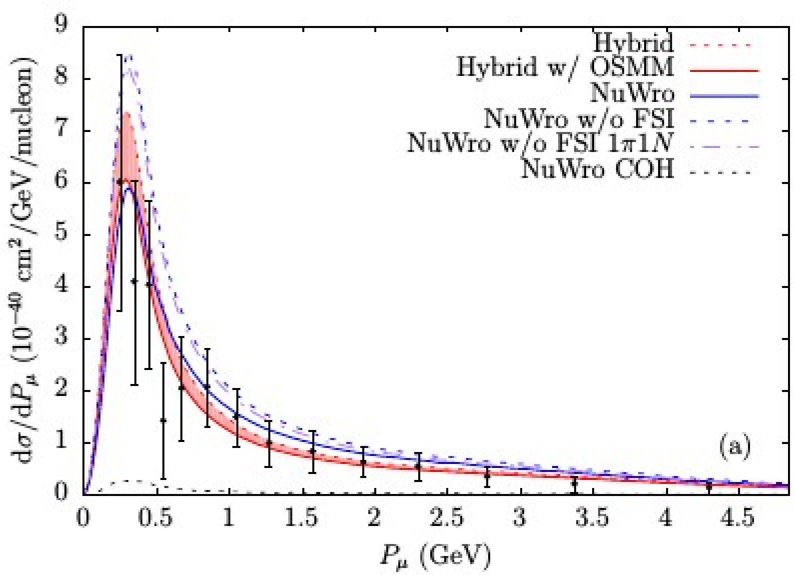

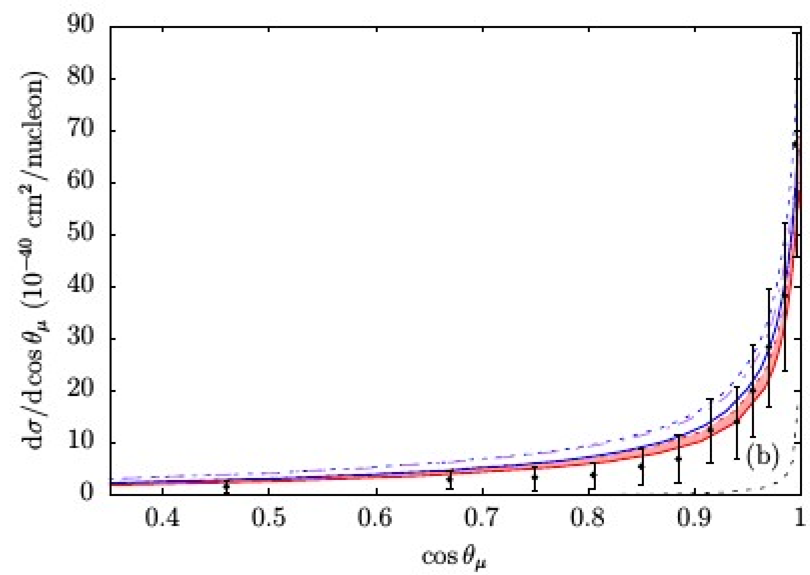

What’s next?

What's next?

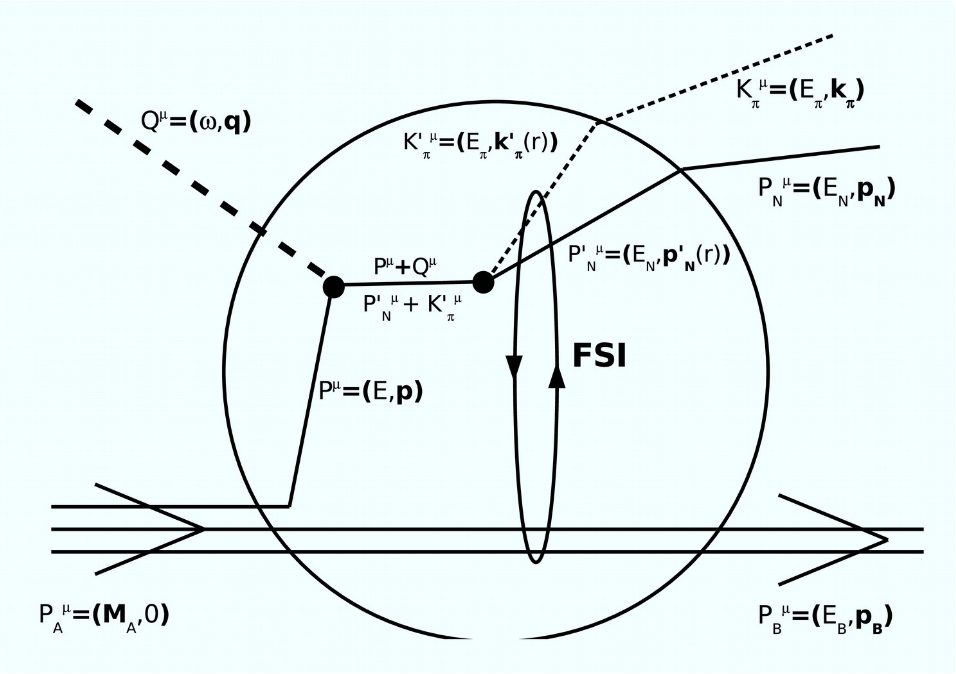

... distortion and absorption of the pion

Conclusions

- ✔ **Microscopic Hybrid model** for single-pion production:
  Low-energy model (resonances + background)
  \+ High-energy model (Regge approach)

  Microscopic: it works at the amplitude level (exclusive predictions)
  Hybrid: it can make predictions from the pion threshold to high invariant mass.

- ✔ Fully r**elativistic and quantum mechanical** framework (relativistic mean-field model).

  Quantum mechanics: wave functions, wave equation, non-factorized
  Relativistic: kinematics and operators

- ✔ **Nuclear effects**:
  Pauli blocking: orthogonality of states
  Distortion: scattered nucleon is the solution in the continuum of the wave equation with mean-field potentials

- ✔ Useful for neutrino-interaction community? **seed for MC neutrino event generators**.

The end...

Grazie per la tua attenzione